Drug Research Program
Division of Pharmaceutical Chemistry and Technology
Faculty of Pharmacy
University of Helsinki
Finland

Synthesis of Antimicrobial Surfaces and Compounds to Target Resistant *Staphylococcus aureus*

Ghada Hassan

DOCTORAL DISSERTATION

To be presented for public discussion with the permission of the Faculty of Pharmacy of the University of Helsinki, in room PIII, Porthania, on February 20th 2021, at 10 am

Helsinki 2021

Supervised by Dr. Vânia M. Moreira, PhD
Laboratory of Pharmaceutical Chemistry
Faculty of Pharmacy
University of Coimbra
Coimbra, Portugal

Center for Neuroscience and Cell Biology
University of Coimbra
Coimbra, Portugal

Professor Jari Yli-Kauhaluoma, PhD
Drug Research Program
Division of Pharmaceutical Chemistry and Technology
Faculty of Pharmacy
University of Helsinki
Helsinki, Finland

Dr. Gustav Boije af Gennäs, PhD
Drug Research Program
Division of Pharmaceutical Chemistry and Technology
Faculty of Pharmacy
University of Helsinki
Helsinki, Finland

Reviewed by Professor John Nielsen, PhD
Department of Drug Design and Pharmacology
Faculty of Health and Medical Sciences
University of Copenhagen
Copenhagen, Denmark

Dr. Antonio Felici, PhD
Vice President, Anti-infectives
Microbiology Discovery Verona
Evotec A.G.
Verona, Italy

Opponent Professor Miguel Castanho, PhD
Faculty of Medicine
University of Lisbon
Lisbon, Portugal

Dissertationes Scholae Doctoralis Ad Sanitatem Investigandam Universitatis Helsinkiensis

ISBN 978-951-51-6995-2 (pbk.)
ISBN 978-951-51-6996-9 (PDF)
ISSN 2342-3161 (print)
ISSN 2342-317X (online)

Unigrafia Oy
Helsinki 2021

You are more than capable to take on the world by storm

ABSTRACT

Antibiotic resistance is a current threat to modern medicine. Not only is it challenging to treat but it also adds considerable costs to the healthcare systems. At the current rate of rising drug resistance, approximately 10 million people will die annually by 2050. The World Health Organization (WHO) has listed the six most threatening pathogens for which new antibiotics and approaches are urgently needed. One of the fastest evolving and most notorious Gram-positive bacteria in the list is *Staphylococcus aureus*. In addition to developing resistance to a vast number of antibiotics, this bacterium can attach to surfaces and form biofilms. This lifestyle allows bacteria to protect themselves from the immune system and impairs treatment. Thus, new innovative approaches and antibacterial agents are needed to fight bacterial resistance.

As microbial adhesion is the first step of biofilm formation, the first aim of this study was to develop novel antibacterial surfaces to hamper the accumulation of antibiotic-resistant microbes. Cellulose is the most abundant natural polymer with various appealing characteristics. It is renewable, biocompatible, biodegradable, and possesses excellent mechanical properties. Cellulose nanofibers are prepared by mechanical disintegration of cellulose. Thin films of cellulose nanofiber can be prepared, and their surface can be modified to provide cellulose with new properties.

Terpenoids such as abietic acid and dehydroabietic acid originating from conifer resin possess antibacterial and antifungal activities. We have previously shown that the amino acid-bearing derivatives of dehydroabietic acid possess antimicrobial properties.

Herein, I report the design and the synthesis of new wide-spectrum contact-active non-leaching antibacterial cellulose nanofiber films by coupling the films with dehydroabietylamine, dehydroabietic acid and their derivatives. Different techniques and measurements were used to study the new biomaterials including contact angle (CA), streaming current measurements, X-ray photoelectron spectroscopy (XPS), atomic force microscopy (AFM), oxygen transmission rate (OTR), water vapor transmission rate (WVTR), scanning electron microscope (SEM), tensile strength, and Young's modulus.

Our unique design rendered four anionic surfaces highly active against the Gram-positive *S. aureus,* including the drug resistant methicillin-resistant *Staphylococcus aureus* (MRSA) and the Gram-negative *Escherichia coli*. The proposed modes of action and the fact that the compounds are based on a new chemical class account for a low potential to spread resistance.

Our most active material **87** was tested against bacterial colonization in both biofilm and artificial dermis models. The bacterial colonization was efficiently prevented in both models. Material **87** proved to be biocompatible as it nurtured fibroblast growth at its surface without causing significant

hemolysis. Our originally designed surfaces represent a new class of renewable biomaterials suitable for biomedical applications.

The second aim of this thesis was to develop a new class of pyrimidine derivatives against *S. aureus* biofilms. From our novel set of pyrimidines, compounds **89**, **99e**, and **100e** displayed potent activities. They inhibited biofilm formation and were active against pre-formed biofilms of *S. aureus* ATCC 25923 and Newman strains with IC_{50} values ranging between 11.6 to 62.0 μM. The compounds were also effective against planktonic cells with minimum inhibitory concentration (MIC) values lower than 60 μM. Only marginal cytotoxicity was revealed against human Hep2 cells at concentrations comparable to their pre-exposure IC_{50} values.

Overall, this study resulted in the synthesis of four new antibacterial biomaterials and 26 new pyrimidine derivatives. This thesis offers novel approaches to target one of the most dangerous antibiotic-resistant bacteria *S. aureus* and efficiently limit its proliferation.

ACKNOWLEDGEMENTS

This research was done at the Division of Pharmaceutical Chemistry and Technology, Faculty of Pharmacy, University of Helsinki, during the years of 2016-2020. I would also like to acknowledge Business Finland, Niemi foundation and the Print-Aid Consortium, European training network for development of personalized anti-infective medical devices combining printing technologies and antimicrobial functionality (H2020-MSCA-ITN-2016, Grant Agreement No 722467) for funding parts of my doctoral studies. I would also like to thank the Doctoral Programme in Drug Research (DPDR) for giving travel grants which made me able to showcase my research in various international conferences.

I would like to acknowledge my amazing supervisors Dr. Vânia M. Moreira, Prof. Jari Yli-Kauhaluoma and Dr. Gustav Boije af Gennäs for their support, guidance, and supervision through my journey. Thank you, Vânia, for always being there despite your tight schedule. Your feedback and advice have always been extremely useful, and I learnt a lot from you.

Thank you Jari for your tremendous support and your trust in me. You have always been available for discussions and I am very proud to have been working in your group. You have a significant impact on increasing my interest in medicinal chemistry.

Thank you Gusse for the opportunity to work with you, it has been a sincere pleasure and I learnt a lot. A special thanks to my work colleagues. Thank you Riky for being an amazing labmate and for teaching me many things. Thank you, Leena, for your guidance and support. Thank you, Erik, for being always available for scientific discussions. Thank you Rali, Paola, Ash, Loïc, Suvi, Sara and Şafak for very many wonderful moments & memories. Thank you Tiina, Laura, Niklas, Mikael, Teppo, Paula, Raisa, Alexi, Mikko and Jayendra, for helping me in multiple ways and for all the fun we had during the conferences. I especially want to thank Markus and Andrew for reviewing this thesis. A special thanks to Heli, Heikki, Milla, Hanna, Johannes and all my friends for their support.

I also want to thank Ebtisam, Ali, Riham, Dina and Amira for always being there and for their support and patience. I am very lucky to be surrounded by people like you.

Helsinki, 2021
Ghada Hassan

CONTENTS

LIST OF ORIGINAL PUBLICATIONS

This thesis is based on the following publications:

I Hassan G, Forsman N, Wan X, Keurulainen L, Bimbo LM, Johansson LS, Sipari N, Yli-Kauhaluoma J, Zimmermann R, Stehl S, Werner C, Saris PEJ, Österberg M, Moreira VM. Dehydroabietylamine-based cellulose nanofibril films: a new class of sustainable biomaterials for highly efficient, broad-spectrum antimicrobial effects. *ACS Sustainable Chemistry & Engineering*. 2019; 7(5):5002-5009.

II Hassan G, Forsman N, Wan X, Keurulainen L, Bimbo LM, Johansson LS, Stehl S, Van Charante F, Chrubasik M, Prakash AS, Johansson LS, Mullen DC, Zimmermann R, Werner C, Yli-Kauhaluoma J, Coenye T, Saris PEJ, Österberg M, Moreira VM. Non-leaching, highly biocompatible nanocellulose surfaces that efficiently resist fouling by bacteria in an artificial dermis model. *ACS Applied Bio Materials*. 2020; 3(7):4095-4108.

III Provenzani R, Galindo PSM, Hassan G, Kallio A, Fallarero A, Yli-Kauhaluoma J. Multisubstituted pyrimidines effectively inhibit bacterial growth and biofilm formation of *Staphylococcus aureus*. Manuscript. This manuscript will also be used in Riccardo Provenzani's and Paola San Martin Galindo's doctoral theses.

The publications are referred to in the text by their Roman numerals.

Author's contributions

I GH designed and optimized a method to functionalize CNF, did all the synthetic work, performed NMR and IR analyses, analysed the results and wrote part of the manuscript together with co-authors under the supervision of VM. NF prepared the CNF films, performed the WCA, AFM and tensile strength measurements, analysed the results and wrote part of the manuscript under the supervision of MÖ and VM. LK helped design and synthesis the compounds and materials and revised the manuscript. L-SJ performed the XPS measurements. XW did the antimicrobial testing and SEM analysis under the supervision of PS. NS did the mass analysis of the compounds. RZ, SS and CW performed the streaming potential measurements. LB did the biocompatibility testing. JY-K revised the manuscript.

II GH synthesized compounds **7a** and **7b**, characterized them using NMR and IR and linked them to the CNF surface. GH also wrote part of the manuscript with co-authors under the supervision of VM. NF prepared the CNF films and performed the WCA and AFM measurements under the supervision of MÖ and VM. LK helped design the compounds and materials and revised the manuscript. L-SJ was responsible for the XPS measurements. XW did the antimicrobial testing and SEM analysis under the supervision of PS. RZ, SS and CW performed the streaming potential measurements. LB did the biocompatibility testing. BJ, MC, AP, DM performed the ToF-SIMS analysis. DM participated in revising the manuscript. FvC and TC did the biofilm and artificial dermis experiments and FvC participated in writing the manuscript. JY-K revised the manuscript.

III GH and RP designed, synthesized and characterized the compounds with equal contribution. PSMG did the microbiology work of the study. AK synthesized a few compounds under the supervision of GH and RP. GH, RP and PSMG wrote the manuscript in equal contribution under the supervision of AF and JY-K.

ABBREVIATIONS

AA	abietic acid
AFM	atomic force microscopy
BS	biosurfactants
CA	contact angle
CAN	ceric ammonium nitrate
CMC	carboxymethyl cellulose
CNF	cellulose nanofibril
DAA	dehydroabietic acid
DCM	dichloromethane
DHAA	dehydroabietylamine
DHF	dihydrofolic acid
DMF	*N*,*N*-dimethylformamide
EPS	extracellular polymeric substances
FTIR	Fourier-transform infrared spectroscopy
MIC	minimum inhibitory concentration
PMP	*p*-methoxyphenyl
RL	rhamnolipids
SAR	structure-activity relationship
SEM	scanning electron microscopy
TBAB	tetra-*n*-butylammonium bromide
TFA	trifluoroacetic acid
THF	tetrahydrofolic acid
TMP	trimethoprim
UV/VIS	ultraviolet/visible (light)
XPS	X-ray photoelectron spectroscopy

1 INTRODUCTION

1.1 NEED FOR NEW ANTIMICROBIALS

The emergence of antimicrobial resistance (AMR) has accelerated over the last decade.[1] Globally, 700,000 patients die every year of resistance-related infections, while in Europe, 33,000 patients die annually because of antibiotic-resistant bacteria.[2] At the current rate of rising drug resistance, approximately 10 million deaths will occur annually by 2050. That will translate into a global economic loss of about USD 100 trillion. A study by Chandy et al. revealed that patients with antibiotic-resistant infections pay USD 700 more than patients who can be treated with first-line antibiotics in India.[3]

In April 2014, the World Health Organization (WHO) published the first global report on antibiotic resistance. The report explained the current situation about the high rates of resistance and stressed that urgent attention is required to avoid the “post-antibiotic era”.[4]

Antibiotics are antibacterial drugs that kill or slow down the growth of bacteria and are used to prevent and treat bacterial infections.[5] They act through various mechanisms of action. They can have an effect on the synthesis of proteins, bacterial cell, ribonucleic acid (RNA), and deoxyribonucleic acid (DNA) or have other specific actions.[6]

Scientists discovered most of the currently used antibiotics during the period of 1940-1970 from natural extracts of microorganisms.[7] Since the discovery of penicillin in 1928, antibiotics have been used beyond treating simple infections. Healthcare professionals used antibiotics in complex medical approaches such as organ transplantations, management of cancer patients and surgical procedures.[8] Antibiotics extend life spans by decreasing the morbidity caused by food-borne and poverty-related infections.[9]

Antimicrobial resistance emerges when antibiotics lose their effect to prevent the growth of bacteria, i.e., bacteria keep on multiplying and growing in the presence of the antibiotic.[10] Unfortunately, resistance has developed to almost all antibiotics known to humans, and to date there are no methods available to reverse the process of antimicrobial resistance.[11] To address this problem, new antimicrobial agents are needed.

The only novel class of antimicrobial compounds discovered in the past 40 years is the oxazolidinones represented by linezolid, released in 2000.[12] Soon after reaching the market, studies identified clinical isolates of *Staphylococcus aureus* and several *Enterococcus* species that were resistant to linezolid.[13] Most of the new antimicrobial agents are analogues of the known compound classes to which resistance has already been developed. Resistance can occur to structurally similar compounds. For example, resistance to tetracycline may incur resistance to minocycline, doxycycline,

chlortetracycline and oxytetracycline.[14] On average only every fifth compound in clinical trials will reach the market.

1.2 MECHANISMS OF ANTIMICROBIAL RESISTANCE

Bacteria use various mechanisms to resist the effect of antibiotics. They can alter or inactivate antibiotics, modify the drug binding site or change cell permeability.[15]

Many bacteria produce enzymes such as β-lactamases, aminoglycoside-modifying enzymes, or chloramphenicol acetyltransferases to modify or inactivate antibiotics. For example, the Gram-negative *E. coli* and *P. aeruginosa* developed resistance to β-lactam antibiotics by producing β-lactamases, which hydrolyze the β-lactam ring present in many antibiotics such as penicillins, cephalosporins, monobactams, and carbapenems.

Other bacteria modify their target site to avoid recognition by antibiotics.[15] They do this, for example, by modifying genes that encode binding proteins. Penicillin-binding proteins (PBPs) are enzymes anchored on the cytoplasmic membrane of the bacterial cell wall. They are involved in the synthesis of peptidoglycan, an essential component of the bacterial cell wall. *S. aureus* can mutate the genes encoding PBPs to form unique penicillin-binding proteins, for example, PBP2a. This mutated protein has a lower affinity for β-lactam antibiotics such as methicillin, which inhibits the synthesis of bacterial cell walls. PBP2a is the most dominant PBP form in the methicillin-resistant *Staphylococcus aureus* (MRSA). Mutated genes can be inherited genetically from mother to daughter bacteria.[10]

Reduction of antibiotic permeability is another strategy used by bacteria to develop antibiotic resistance.[15] The bacterial cell envelope has a complex structure that regulates the molecular traffic between the cell and its environment. The cell envelope of Gram-negative bacteria differs from that of Gram-positive bacteria. It consists of an outer membrane followed by a peptidoglycan cell wall and an inner cell membrane (Figure 1).[16] The outer membrane is a distinguishing feature of Gram-negative bacteria and is lacking in Gram-positive bacteria. The outer membrane is composed of glycolipids mainly lipopolysaccharide. The lipid portion acts as endotoxin and can trigger various life-threatening physiological reactions in humans. The main function of the outer membrane is to act as a protective barrier making Gram-negative bacteria more resistant to antibiotics compared to Gram-positive bacteria.

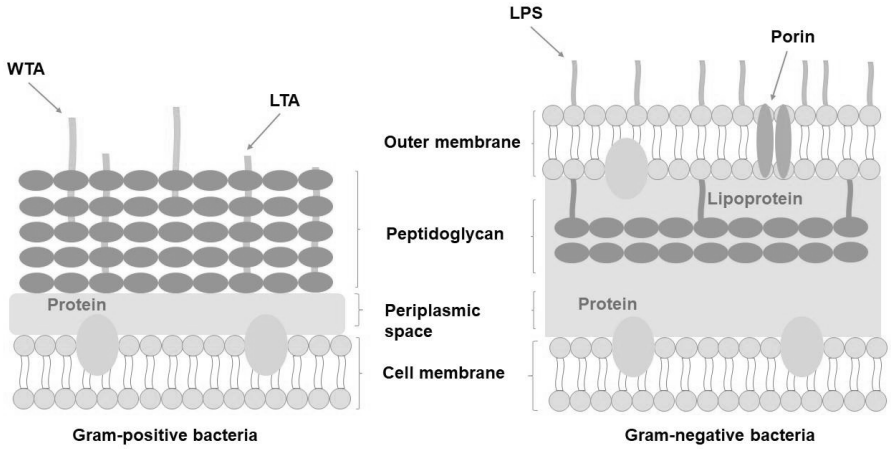

Figure 1 Difference in cell envelope between Gram-positive and Gram-negative bacteria. LPS, lipopolysaccharide; WTA, wall teichoic acid; LTA, lipoteichoic acid (adapted from Silhavy et al. 2010).[16]

The outer membrane of Gram-negative bacteria contains proteins known as porins.[15] These proteins provide aqueous channels and facilitate the passive transport of small hydrophilic antibiotics. *P. aeruginosa* developed resistance to the antibiotic imipenem by reducing the expression of porin protein OprD which reduced drug influx into the cell. *Acinetobacter baumannii* became resistant to the antibiotics imipenem and meropenem by decreasing the expression of 29 kDa outer membrane protein. This protein is involved in transporting molecules across the outer membrane of the bacteria.

Antibiotics larger than 600 Da, such as vancomycin and daptomycin, cannot penetrate the envelope of Gram-negative bacteria.[17] Thus, the outer membrane of Gram-negative bacteria hampers the development of novel antibiotics.

The main part of the cell envelope found in both Gram-positive and Gram-negative bacteria is the peptidoglycan layer.[16] As Gram-negative bacteria are gifted with the outer membrane, their peptidoglycan layer is relatively thin consisting of one to few layers and is few nanometers thick. On the contrary, Gram-positive bacteria have thick and multi-layered peptidoglycan, around 30–100 nm thick. Within their thick peptidoglycan layer, Gram-positive bacteria have long anionic polymers known as teichoic acids. They are composed mainly of glycerol phosphate, glycosyl phosphate, or ribitol phosphate repeats and account for 60% of the mass of the cell walls of Gram-positive bacteria. They are divided into two main groups, wall teichoic acids, covalently attached to peptidoglycan, and lipoteichoic acids, attached to the head groups of membrane lipids.

In addition to teichoic acids, the surfaces of Gram-positive bacteria contain a variety of proteins.[15] As these bacteria lack an outer membrane to contain extracellular proteins, all the proteins exist in or near the membrane. The

peptidoglycan layer is a target for many antibiotics, which cause cell lysis. However, bacteria can protect themselves by inactivating the antibiotics, as in the case of producing β-lactamases to target β-lactam antibiotics.

Efflux pumps are transport proteins localized in the cell membrane of both Gram-positive and Gram-negative bacteria.[18] They are used by bacteria to remove antibiotics from their intracellular compartment. Most of the efflux pumps are multidrug transporters able to expel a wide range of antibiotics at a high rate. The synergistic effect of the outer membrane barrier and the efflux pumps is a key for resistance in many bacteria.[15] For example, multidrug-resistant *Enterobacter aerogenes* overexpresses its AcrAB efflux pumps and simultaneously decreases the expression of porins. This results in lower antibiotic permeability and more effective resistance.

Bacteria have developed various antibiotic resistance mechanisms. The main mechanisms include modification of drug targets, enzymatic inactivation, and limiting cell permeability through porin loss or overexpression of efflux pumps. Bacteria can resist a wide range of antibiotics by developing multiple resistant mechanisms simultaneously causing hard to treat infections. In addition, bacteria prefer to live in communities, attach to surfaces and embed themselves in a self-produced matrix.[15] This lifestyle is known as biofilm and it offers the bacteria many advantages. The matrix of the biofilm improves cellular communication and provides a mechanical shield by acting as a permeability barrier to antibiotics, thus increasing resistance. Taken together, novel tools are needed to prevent and treat infections caused by resistant bacteria and disrupt the biofilm structure.

1.3 INFECTIONS RELATED TO ANTIMICROBIAL RESISTANCE

Antimicrobial resistance is becoming a global life threat.[19] In particular, the so-called ESKAPE pathogens *Enterococcus faecium*, *S. aureus*, *Klebsiella pneumoniae*, *Acinetobacter baumannii*, *Pseudomonas aeruginosa*, and *Enterobacter* species and their resistant forms are of great concern.[20] For example, a global pandemic of resistant *S. aureus* kills more Americans per year than HIV, emphysema, Parkinson's disease and homicide combined.[21] The most serious bacterial infections happen in healthcare environments such as care homes and hospitals. The patients at greater risk of healthcare-associated infections are immunocompromised and invasive surgery patients.[22] Infections related to the use of medical devices pose an especially significant financial burden. Catheter-related urinary tract infections, lower respiratory tract infections and infections related to surgeries are the most common.

In addition to being challenging to treat, antimicrobial resistance adds considerable costs to the healthcare systems.[23] Patients with persistent infections have prolonged hospital stays by 6.4-12.7 days. When the first- and

second-line antibiotics are not effective anymore, doctors prescribe the so-called antibiotics of last resort that are generally very expensive. A study by Thorpe and colleagues analysed data from the Medical Expenditure Panel Survey[24] to estimate extra costs of treating resistant infections.[25] They estimated an additional cost of USD 1,383 per patient due to resistant bacterial infection. Currently, the most notorious Gram-positive resistant bacterium is *S. aureus*.[26] It is a spherical bacterium, which clusters in a grape-like form. It is 1 µm in diameter and can exist asymptomatically on many parts of the human body including the mucous membrane and skin.[27]

1.4 EXAMPLES OF ANTIMICROBIAL-RESISTANT BACTERIA

1.4.1 MRSA

Methicillin-resistant *S. aureus* (MRSA) is any strain of *S. aureus* that has developed resistance towards the broad-spectrum β-lactam antibiotics such as cloxacillin, methicillin and flucloxacillin.[28] MRSA has developed resistance towards many antimicrobial agents including fluoroquinolones, aminoglycosides, cephalosporins, macrolides and β-lactams as well as vancomycin, trimethoprim-sulfamethoxazole and tetracycline.[29] In the USA, 19,000 people die every year due to MRSA.[30]

The emergence of resistant *S. aureus* species developed in a series of steps. In the 1940s, the number of infections related to penicillin-resistant *S. aureus* increased in healthcare sectors.[29] This strain was able to develop penicillinase, which hydrolyzes the strained β-lactam ring of penicillin. The next step followed when methicillin was introduced in the 1960s. This time the mechanism of resistance differed from the penicillinase-mediated resistance. It was much broader and included resistance to all β-lactam class antibiotics, such as carbapenems, cephalosporins and penicillin. By the mid-1980s the MRSA pandemic started in hospitals and healthcare centers, resulting in the increased use of vancomycin. Vancomycin was the last remaining antibiotic to which MRSA was susceptible. The intensive use of vancomycin resulted in the emergence of vancomycin-intermediate *S. aureus* (VISA).

Currently, MRSA is one of the fastest evolving bacteria, causing a wide range of infections from skin disease to serious endocarditis.[31] Various sequelae can result from MRSA infection such as chronic wound infection, septic conditions, bloodstream infection and ventilator-associated pneumonia.[32] MRSA is the leading cause of chronic infections for indwelling medical devices.[33]

MRSA can asymptomatically colonize in its host (almost 30% of humans are carriers), where it transmits easily through skin contact.[29] MRSA infection is divided into two categories based on the genetic makeup: hospital-acquired infection and community-acquired infection (HA-MRSA and CA-MRSA,

respectively).[30] In the community setting, MRSA causes skin and lung infections, which can become severe if left untreated.[34] However, in healthcare settings, MRSA causes more serious infections. Bloodstream and surgical site infections and pneumonia are the most common. The infection risk increases in crowded places, especially with frequent skin contact or through the sharing of personal items.

HA-MRSA is a vigorous MRSA type that infects hospitalized immunocompromised patients.[35] Lopes and colleagues did a cross-sectional study, where they tested the saliva and nasal secretion of 100 nurses providing care for immunocompromised HIV patients.[36] They detected *S. aureus* in 43% of the tested subjects. A bacterial resistance study showed that 92% of *S. aureus* was resistant to penicillin, 45% to erythromycin, 42% to clindamycin and 15% to oxacillin.

The biggest challenge in treating HA-MRSA is its ability to grow within biofilms that protect them against different therapies.

Bacteria can exist in three different states.[37] The first state is the planktonic single-cell state that causes acute infections. Antimicrobial agents can easily eradicate planktonic cells. In the second state, bacteria form communities in a self-produced matrix and this bacterial lifestyle is called biofilm that causes hard-to-treat infections. The treatment of biofilms remains ineffective with conventional antimicrobial agents. The third state is dispersed and corresponds to a stage between planktonic and biofilm states. This state facilitates biofilm spreading and the transmission of infection.

1.4.2 BIOFILM

Biofilms are communities of microorganisms that attach to each other and to living or non-living surfaces.[38] The adherent cells live in a self-produced slimy extracellular polymeric matrix. This lifestyle allows the microorganisms to share nutrients and survive physicochemical aggression such as desiccation, acidity, heavy metals, salinity, phagocytosis and antibiotics.[10]

Biofilm formation involves several phases (Figure 2).[39,40] The first phase requires cells to attach reversibly onto a surface. Cells adhere initially through hydrophobic interactions or van der Waals forces.[41,42] In favorable conditions, bacteria anchor themselves irreversibly to the surface using attachment cells such as pili and produce biofilm matrix components forming microcolonies. The extracellular matrix (ECM) protects the biofilm from stress conditions, and it contains a mixture of lipids, proteins, nucleic acids and polysaccharides.[37] The matrix secretion continues until the third stage of the biofilm, where it appears as a three-dimensional tower-like structure.

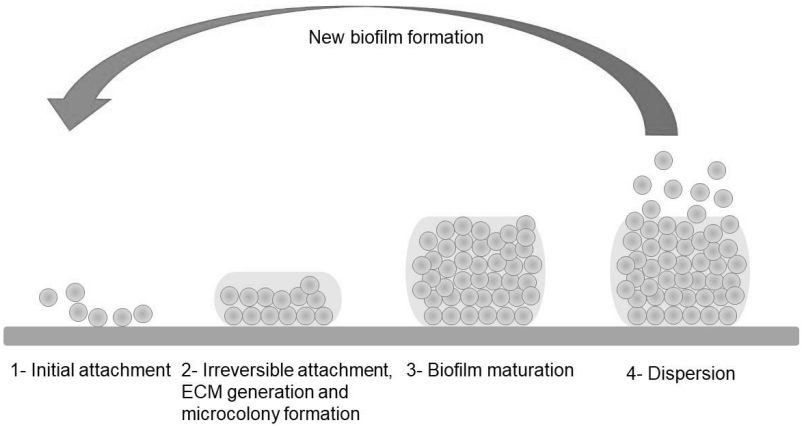

Figure 2 *Demonstration of S. aureus biofilm formation. Biofilm formation starts with initial attachment, which develops into irreversible attachment, ECM generation and microcolony formation. Bacteria multiply and biofilm becomes mature after which cells disperse to a new surface to form a new biofilm (adapted from Lu et al. 2019).*[39]

During colonization, bacterial cells communicate through a system known as quorum sensing (QS). During this process bacteria share information using small signaling molecules, which allow them to grow and mature into large cellular aggregates. Studies have shown that the QS systems are different between Gram-negative and Gram-positive bacteria.[43] Gram-negative bacteria use mainly *N*-acylated homoserine lactone (HSL) molecules for communication (Figure 3) while Gram-positive bacteria use modified oligopeptides. The mature biofilm forms water channels to efflux waste and influx nutrients. In the final stage, the mature bacteria disperse to new niches to start a new biofilm.

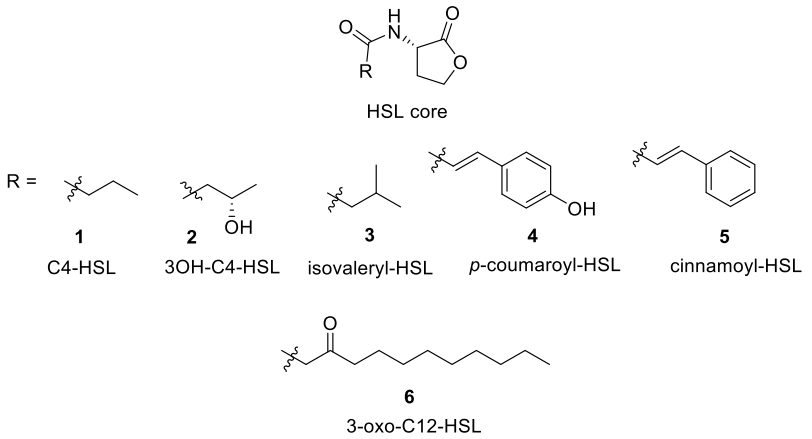

Figure 3 *Examples of the most common class of signalling molecules produced by Gram-negative bacteria. They have N-acylated homoserine lactone ring and different length carbon acyl chain (adapted from Papenfort and Bassler 2016).*[44]

Biofilm cells are physiologically different from planktonic cells of the same bacterial species.[45] Planktonic cells switch to biofilm mode after a phenotypic shift in behavior and gene regulation.[46] Typically, biofilms are formed in response to different factors such as recognition of an attachment site, exposure to sub-inhibitory doses of antimicrobial agents or nutritional cues.[45,47] It is estimated that over 80% of human bacterial infections are biofilm-related.[48]

In most cases, antimicrobial agents reduce biofilm mass but do not eliminate the entire biofilm. A subpopulation of bacterial cells (less than 1%) known as “persister cells” enter a dormant state to escape the effect of antimicrobials without genetic modification.[10] After the end of antibiotic exposure, persister cells resume growing to form a new biofilm. As persister cells survive antibiotics, they can cause infection recurrence even after the administration of high concentrations of antibiotics for a long time. Thus, the reason of biofilm resistance toward antibiotics relies mainly on the presence of such persister cells. Studies of dose-dependent killing of *P. aeruginosa* biofilm have shown the presence of persister cells as a small subpopulation of bacterial cells completely tolerant to antibiotics such as ciprofloxacin and ofloxacin.[49]

Examples of persistent infections comprise of endocarditis caused by staphylococcal biofilms and medical device-associated infections, such as *P. aeruginosa* lung infections and streptococcal otitis media. These infections can be cured or alleviated partially but require prolonged treatment periods.[22] Moreover, the biofilm structure protects the bacteria against the immune system as it impairs the activation of phagocytes and complement systems causing a 1000-fold resistance towards conventional antibiotics.[37] Studies have shown that biofilm cells undergo a higher rate of mutation compared to planktonic cells. That results in a 10-fold increase in the ability of the bacteria to transfer plasmid carrying resistance genes.[50]

2 REVIEW OF THE LITERATURE

2.1 ANTIMICROBIAL AND ANTI-BIOFILM AGENTS

The common way of treating antibiotic-resistant biofilm infections is through the administration of higher doses of antimicrobial agents or by using alternative antimicrobial agents as such or in combination with other agents. Ideally, they should penetrate the biofilm matrix and be effective towards the bacterial species forming the biofilm.[37] The use of antimicrobial agent combinations is preferred as different mechanisms of actions strengthen the overall effect of treatment. Antimicrobial agents are divided into various categories depending on their modes of action. They can inhibit the formation of the polymer matrix, suppress the adhesion of bacterial cells onto surfaces or decrease the production of virulence factors by disturbing the QS network.[43] They can also interfere with the synthesis of deoxyribonucleic acid (DNA) and ribonucleic acid (RNA) or interfere with the bacterial cell wall formation. Other modes of action include lysis of the bacterial membrane, inhibition of the bacterial metabolic pathways and protein synthesis.[11]

2.1.1 THE ANTIMICROBIAL ACTIVITIES OF RESIN TERPENOIDS WITH FOCUS ON DEHYDROABIETIC ACID

Conifers are one of the oldest plant species found on Earth with the earliest fossil dating back to 300 million years ago.[51] Conifers have a highly evolved defence system, which protects them from outer invaders. When wounded, the trees secret viscous oleoresin, which traps the invading insects and seals the tree wound.[52] Resin consists mainly of volatile and non-volatile terpenes. Terpenes have a cycloaliphatic structure made of isoprene units assembled to each other in various ways. The common terpenes are classified mainly based on their carbon units as monoterpenes (C_{10}), sesquiterpenes (C_{15}), diterpenes (C_{20}), sesterpenes (C_{25}) and triterpenes (C_{30}).[53] When terpenes are modified by removing methyl groups or adding oxygen atoms, they are referred to as terpenoids. Under natural conditions, volatile terpenes evaporate from resin, leaving behind a solid portion of non-volatile components, comprising diterpenoids, known as rosin.

Studies have shown that terpenes and terpenoids possess antibacterial and antifungal activities.[54,55,56] Fallarero et al. screened a library of natural and semi-synthetic abietane-type diterpenoids against *S. aureus* biofilms.[57] The most active compounds were nordehydroabietylamine (**7**), (+)-dehydroabietylamine (DHAA) (**8**) and (+)-dehydroabietic acid (DAA) (**9**) (Figure 4). They prevented biofilm formation (in the pre-exposure assay) and disrupted pre-formed biofilms (in the post-exposure assay) in the micromolar range. DAA had the highest selectivity towards the tested biofilms. Non-

specific cytotoxicity studies on three mammalian cell lines revealed that DAA was well tolerated.

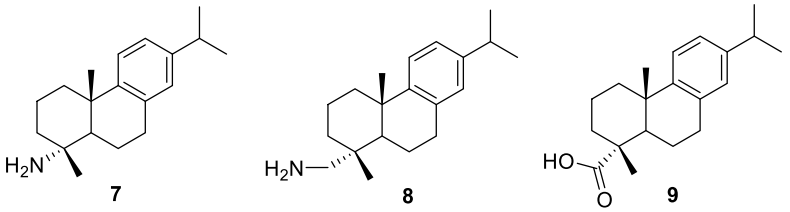

Pre-exposure (IC_{50} = 116 µM)	Pre-exposure (IC_{50} = 34 µM)	Pre-exposure (IC_{50} = 17 µM)
Post-exposure (IC_{50} = 294 µM)	Post-exposure (IC_{50} = 81 µM)	Post-exposure (IC_{50} = 74 µM)

*Figure 4 Structures of nordehydroabietylamine (**7**), DHAA (**8**) and DAA (**9**) studied against S. aureus biofilms in the pre- and post-exposure assays.*

Different studies have focused on the modifications of diterpenoids to improve their bioactivities.[58] So far, DAA is the most extensively studied.

To enhance the biofilm potency of DAA, Manner and colleagues modified rings A and B of its diterpenoid core and combined it with different amino acids.[56] They screened the compounds against the biofilms of two different *S. aureus* strains in pre- and post-exposure assays. The initial screening was done at 400 µM and the active hits were retested at 100 µM concentration. The group identified the best potent anti-biofilm compound **11** (Figure 5) with minimum inhibitory concentration (MIC) values of 15 µM and 20 µM for *S. aureus* ATCC 25923 and Newman, respectively. Mechanism-of-action studies revealed that the compound **11** likely targets the bacterial cell membrane and disrupts the formed biofilm. The compound showed no statistically significant reduction in HL cells (originating from the human respiratory tract) when tested up to 100 µM proving to be non-cytotoxic to human cells at the concentrations needed to inhibit the formation of bacterial biofilms.

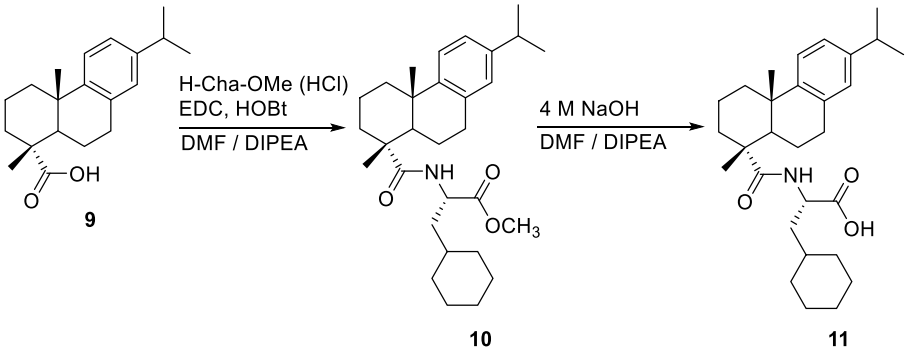

*Figure 5 The synthesis route of the most active compound **11** identified by Manner et al. 2015.*

In a mission to target different strains of MRSA and methicillin-susceptible *S. aureus* (MSSA), Chabán and colleagues developed a new series of abietatrienes from DAA by modifying the C13 position of ring C.[59] The library of 29 compounds was tested against the following bacterial strains: MRSA ATCC 33592, LA-MRSA LGA251(ST425-XI), HA-MRSA ST5-SCCmecI, MSSA ATCC 6538 and ST30-t021. The research group used three antibiotics, gentamicin, vancomycin and penicillin as reference substances. Based on the displayed activity, four compounds (Figure 6) were chosen for further testing against 12 MRSA and 9 MSSA strains. Compound **13** showed potent antibacterial activity with low MIC values against all the tested strains followed by compound **12**. Compound **15** was active against all but one strain, while **14** was active against 6 MRSA strains. Compound **13** was tested against human erythrocytes at 181 μM, a value much higher than its MIC, and showed no cytotoxicity. The group concluded that an oxime moiety at C13 combined with a free hydroxyl group at C12 enhances the activity of DAA towards different *S. aureus* strains.

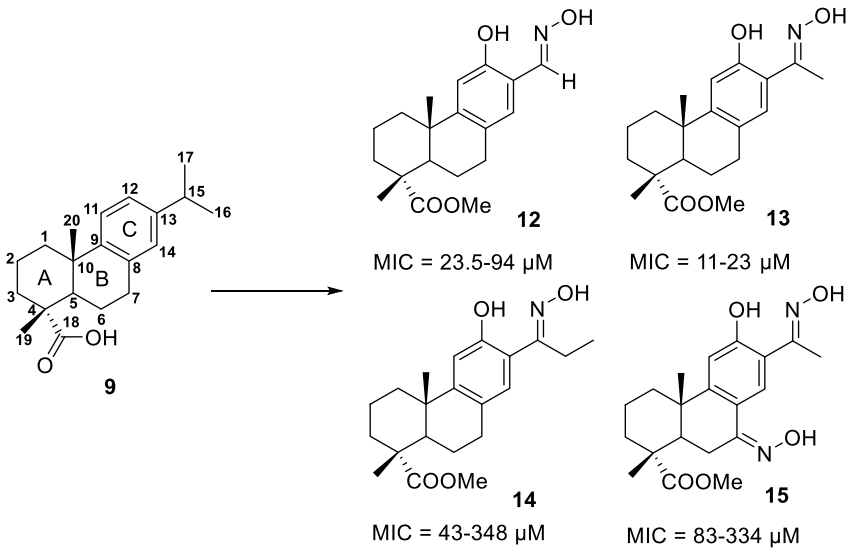

Figure 6 The structure of the most active DAA derivatives synthesized by Chabán et al. 2019 and their antibacterial activities.

Liu et al. synthesized a series of 12-oxime and *O*-oxime ether derivatives of DAA by modifying the C12 substituent and tested them for their anti-staphylococcal activity.[60] The compounds were tested against *S. aureus* and five multidrug-resistant strains (NRS-1, NRS-70, NRS-100, NRS-108, and NRS-271). The aromatic oximate **18** (Table 1) was the most active against *S. aureus* Newman with low MIC values ranging between 0.8 and 1.6 μM. In comparison, the parent compound DAA had moderate activity against Newman strain with MIC values ranging between 41 and 66 μM. The three compounds **16**, **17** and **19** were the most potent against the five multidrug-

resistant *S. aureus* strains. The research group concluded that the presence of an oxime functionality at C12 enhanced the activity of DAA against multidrug-resistant *S. aureus*.

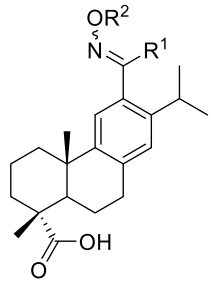

16 - 19

Table 1 *Structure of DAA oximate derivatives, their MIC values against S. aureus Newman strain and their MIC ranges against all the tested bacterial strains.*

Compound	R1	R2	MIC values (μM) *S. aureus* Newman	MIC values (μM) All strains
16	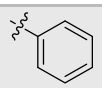	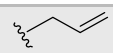	2.7-5.4	2.7-6.8
17	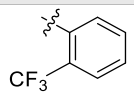	H	3.2-6.4	3.2-6.4
18	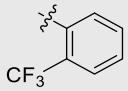	CH3	0.8-1.6	0.8-24.9
19	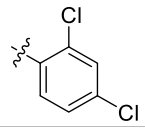	H	3.2-6.4	3.2-6.4

In another study, derivatives of DAA were synthesized and their activities were tested against a filamentous fungus, yeasts, and bacteria (Figure 7).[61] Modifications were done using different configurations on the asymmetric carbon atoms of the A/B ring junction and different functional groups at C18, C7 or C12, without an isopropyl group at C13. All compounds showed activity against the fungus *Trichophyton mentagrophytes*. Compounds **20** and **23** showed significant relative inhibition (RI) of 100% while compounds **25** and **29** showed RI of 91% and 90%, respectively. The absence of the isopropyl group at C13 and the presence of hydroxyl groups at C7 or C12 enhanced the activity. The stereochemical differences were not significant for the activity as shown with compounds **25** and **29**.

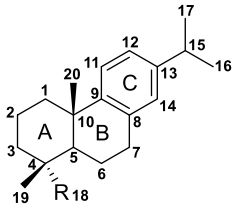

20- R=CO_2Me
21- R=CH_2OH
22- R=CHO

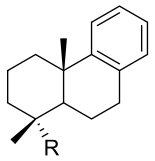

23- R=CO_2H
24- R=CO_2Me
25- R=CH_2OH
26- R=CHO

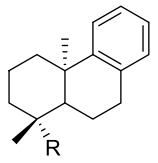

27- R=CO_2H
28- R=CO_2Me
29- R=CH_2OH
30- R=CHO

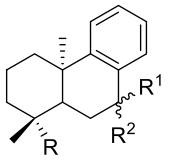

31- R=CO_2Me, R^1, R^2=O
32- R=CH_2OH, R^1=OH, R^2=H
33- R=CHO, R^1, R^2=O

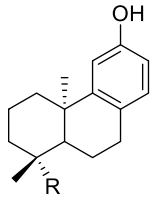

34- R=CO_2Me
35- R=CH_2OH

Figure 7 The structure of DAA derivatives synthesized by Gigante et al. 2002.

Only compounds with a formyl group at C18 showed activity against several *Candida* strains. Compound **30** exhibited significant antifungal activity with MIC values 26.9-53.8 μM. The activity was improved more than two-fold with a ketone carbonyl present at C7 as **33** had MIC values 12.7-25.4 μM.

None of the compounds were active against the Gram-negative bacteria *P. aeruginosa* and *Serratia marcescens*. Compounds containing hydroxyl or formyl groups at C4 such as **21**, **22**, **25**, **29** and **30** showed good activity against *S. aureus* with MIC values of 5.6, 5.6, 6.5, 6.5 and 6.6 μM, respectively. The parent compound DAA was not active below a 40 μM concentration when tested against *S. aureus*. The different stereochemistry and the presence or absence of the isopropyl group at C13 did not affect the activity. It was concluded that a simple derivatization of DAA had a significant impact on the antimicrobial activity of its derivatives.

2.1.2 THE ANTIMICROBIAL ACTIVITIES OF PYRIMIDINES

Pyrimidines are six-membered aromatic heterocyclic compounds with two nitrogen atoms at 1,3-positions of the ring.[62] Substituted pyrimidines have essential functions in all living organisms and human metabolism. They are constituents of human RNA and DNA.

Different pyrimidine-based compounds show remarkable antimicrobial activities (Figure 8). Trimethoprim (TMP) is a marketed trisubstituted pyrimidine-containing drug, which binds to dihydrofolate reductase and inhibits the conversion of dihydrofolic acid (DHF) to tetrahydrofolic acid (THF), inhibiting bacterial DNA synthesis.[63] It is used to treat acute urinary tract infection.[64] Recently, different analogues of trimethoprim have been developed in the search for new antibiotics with better pharmacological profiles. Brodimoprim is another trimethoprim analogue with a similar antibacterial spectrum to its parent compound.[65] It is also a selective inhibitor of bacterial dihydrofolate reductase (DHFR) but has a longer half-life compared to trimethoprim.

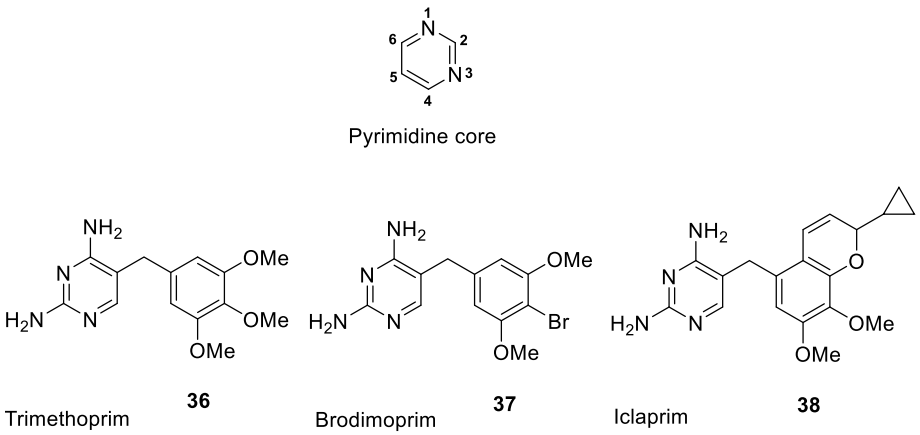

Figure 8 Pyrimidine core and antibacterial trisubstituted and tetrasubstituted pyrimidines.

Iclaprim is a trisubstituted pyrimidine and an optimized trimethoprim analogue.[66] Like its parent compound, iclaprim selectively inhibits the synthesis of dihydrofolate reductase, essential for the synthesis of bacterial RNA, DNA and proteins. It was mainly developed to gain activity against TMP-resistant strains and other resistant bacteria.[67] Iclaprim has reached phase III clinical trials for the treatment of acute skin infections and Gram-positive hospital-acquired pneumonia. A study evaluated the activity of iclaprim against MRSA in an *in vitro* pilot study.[66] The study was conducted using 61 different MRSA isolates, which were not susceptible to different antimicrobial agents including vancomycin, daptomycin and linezolid. As demonstrated in Table 2, iclaprim exhibited potent activity in the micromolar range against all the isolates. Furthermore, the bactericidal activity of iclaprim was studied using a time-kill assay, which showed that the molecule is fast-acting. It exhibited bactericidal activity against the different MRSA phenotypes at 4-8 h. The research team concluded that iclaprim is highly active and rapidly acting. However, the iclaprim marketing approval application was withdrawn from the European Medicines Agency.[68] The scientific evidence failed to prove that the

drug was as good as comparator antimicrobial agents. Furthermore, resistance has already been developed before it is in general use.

Table 2 The antimicrobial activity of iclaprim against different MRSA isolates.

MRSA phenotype	MIC range (μM)
Daptomycin non-susceptible (n=7)	0.34-22.57
Linezolid non-susceptible (n = 26)	0.08-2.82
Vancomycin intermediate (n = 23)	0.71-22.57
Vancomycin resistant (n = 5)	0.71-22.57

As demonstrated above, the most common and fastest strategy for developing new antimicrobial agents is mainly through modifying the existing analogues.[69] However, the new analogues tend to have the same macromolecular target and similar structure to that of the parent compound. The absence of structural variation often leads to accelerated antimicrobial resistance. Taken together, current studies focus on designing and synthesizing novel pyrimidine derivatives to target resistant bacteria.

Veeraswamy and colleagues synthesized a library of novel pyrido[2,3-*d*]pyrimidines and screened them for their antibacterial activity against seven different Gram-positive and Gram-negative bacteria.[70] Compounds **40**, **41**, **45** were active against all tested bacteria (Table 3). Compound **42** was active against the Gram-positive *S. aureus* and the Gram-negative *Klebsiella planticola* with MIC values 16.5 and 32.9 μM, respectively. Compound **43** exhibited specific activity towards *S. aureus* only with MIC value 15.4 μM. Compounds **39** and **44** had specific activity towards *K. planticola*. The rest of the compounds were inactive even when tested at higher concentrations.

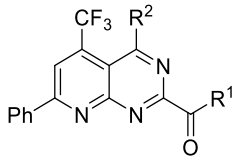

39 - 45

Table 3 The chemical structures of the most active pyrido[2,3-d]pyrimidines and their antimicrobial activities.

Compound	R^1	R^2	MIC (μM)
39	NHC_2H_5	C_6H_5	73.9
40	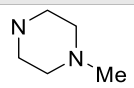	C_6H_5	16.4-65.4
41	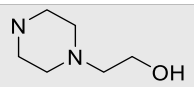	C_6H_5	15.4-61.5
42	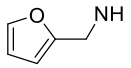	C_6H_5	16.5-32.9
43	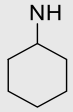	4-MeO-C_6H_4	15.4
44		4-MeO-C_6H_4	32.6
45	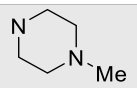	4-MeO-C_6H_4	15.4-30.8

The Sec pathway is the major route responsible for secreting protein across the bacterial cytoplasmic membrane.[71] A key component of this pathway is ATPase SecA, which mediates protein translocation. Jang et al. synthesized a novel series of thiazolo[4,5-*d*]pyrimidines and assessed their ability to inhibit the intrinsic SecA ATPase activity of *S. aureus* and *E. coli*. The compounds were tested at 200 μM. The most active compounds were **46** and **47**, as they inhibited the intrinsic *E. coli* SecA ATPase activity by 76% and 70%, respectively (Figure 9). The IC_{50} values of **46** and **47** were found to be 135 μM and 197 μM, respectively. These compounds showed weak activity towards *S. aureus*.

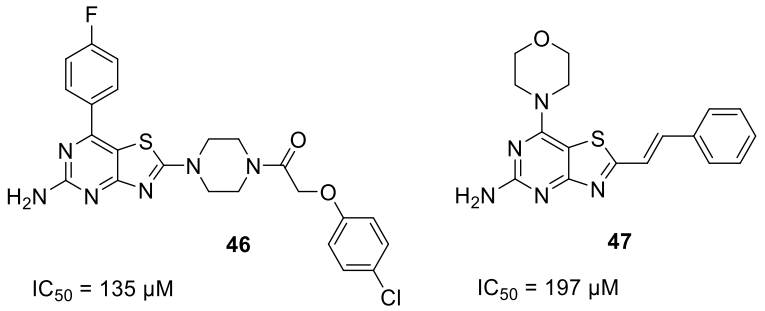

Figure 9 *The chemical structures of the most active compounds **46** and **47**.*

In another study, a series of 6-substituted 4-aminopyrazolo[3,4-*d*]pyrimidines were prepared and screened against four Gram-positive and three Gram-negative bacteria (Table 4).[72] Most of the tested compounds exhibited significant activities toward the Gram-positive *Streptococcus pyogenes* and the Gram-negative *P. aeruginosa*. The activity of the compounds was ranked **48** > **53** > **50** > **51** > **52** > **54** > **49**. Compound **48** had broad-spectrum activity and was the most active with MIC values ranging between 0.1 and 17.1. The aliphatic methyl substituent showed the most activity followed by the monosubstituted phenyl and the disubstituted phenyl, respectively. Among **49**-**54**, the 4-chlorophenyl substituted **53** was the most active while the presence of residual chlorine substituent in **54** decreased the activity.

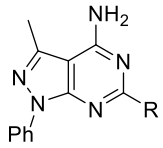

48 - **54**

Table 4 *The chemical structure and the MIC values of **48**-**54** against the most relevant bacterial strains, Streptococcus pyogenes and P. aeruginosa in mM.*

Compound	R	*S. pyogenes* (mM)	*P. aeruginosa* (mM)
48	CH_3	0.3	2.1
49	C_6H_5	N.A.[a]	1.7
50	4-CH_3-C_6H_4	1.6	1.6
51	4-Br-C_6H_4	0.1	1.4
52	4-NO_2-C_6H_4	0.7	1.5
53	4-Cl-C_6H_4	1.5	3.1
54	2,4-di-Cl-C_6H_3	1.38	2.8

[a]N.A. = Not active

In a recent study, Bai et al. synthesized a library of novel pyrimidine derivatives and screened them for their antibacterial activities against *S. aureus*, *Streptococcus mutans*, *E. coli* and the fungus *C. albicans*.[73] Compounds **55**, **57**, **58**, **59** and **60** had good activity towards the tested microbes (Figure 10). Compound **56** was identified as the most active one. It was apparent that the position of the 2,4-dichlorobenzyloxy group with respect to the benzene ring affected the activity as **56** was more active than **57**. In addition to that, the position of the 2,4-dichloro substituent on the benzyloxy substituent influenced the activity, as **56** was more active than **55**. Molecular docking simulation revealed that **56** interacts well with the active cavities of dihydrofolate reductase, an essential enzyme in the folate synthesis pathway. The cytotoxicity evaluation of **56** and **57** in human liver cells proved that they were not cytotoxic.

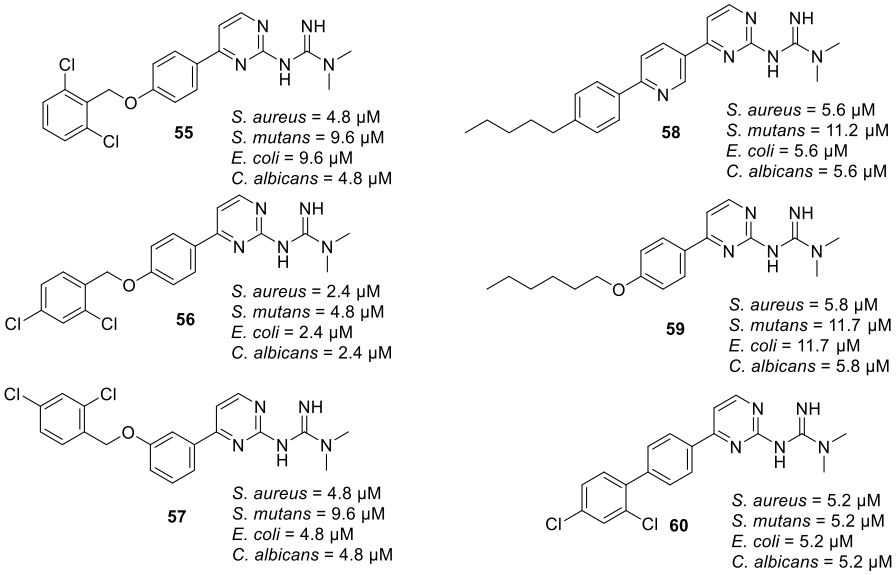

Figure 10 The chemical structures and MIC values of the most active pyrimidine derivatives against S. aureus, S. mutans, and E. coli as well as antifungal activities (*C. albicans*).

As antimicrobial resistance continues to rise, new antibiotics and other antimicrobial agent classes and innovative treatment approaches of infectious bacterial diseases are needed. Some pyrimidine derivatives have successfully reached the market and have proven to be effective and safe. A variety of studies yielded new promising scaffolds with potent broad-spectrum antimicrobial activities. This highlights the value of pyrimidines as promising starting materials for the development of new antimicrobial agents.

2.2 DESIGN PRINCIPLE OF ANTIMICROBIAL SURFACES

Contamination of surfaces with resistant bacteria represents a great challenge. Bacteria prefer to colonize an existing surface rather than dwell in the planktonic state.[74] Bacteria attach to surfaces to enhance membrane stability and reduce the net negative charge of the cells.[75] Surfaces also help protect the cells against environmental threats.[76] Bacteria can colonize different materials including fluorinated materials, glass, stainless steel, aluminum and different organic polymers. They can also attach onto surfaces that should resist attachment by depositing a layer of protein, which masks the functional groups that could reduce cell attachment. Bacterial colonization causes transmission of infection from surface to surface and to humans.[77] This is problematic in a wide range of areas as it reduces the operational function of surfaces and devices. Examples of affected surfaces include petroleum pipelines, textiles, medical implants and aquatic flow systems.[78,79] For example, the attachment of bacteria onto biomedical and indwelling devices and surgical implants introduces pathogenic bacteria into the human body.[80]

Many physical and chemical factors are known to affect bacterial attachment onto surfaces. Examples include hydrophobicity, surface charge, chemical environment and surface topography (Figure 11). van der Waals forces and interfacial electrostatic interactions clearly influence the interaction between bacterial cell walls and surfaces.

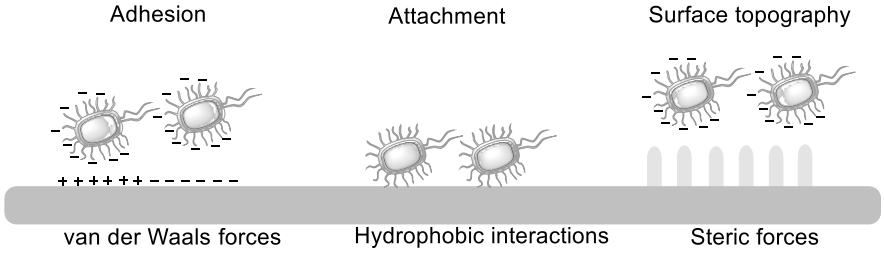

Figure 11 Factors guiding the initial attachment of bacteria to a surface. The initial attachment is governed by van der Waals interactions to overcome energy barriers. After overcoming this obstacle, hydrophobic-hydrophobic interactions occur between the bacteria and the substrate. At this stage, bacterial curli, fimbriae, flagella, and pili interact with the surface. Hydrophobic cells attach strongly to hydrophobic surfaces. Substrate surface topography physically influences bacterial adhesion (adapted from Renner and Weibel 2011).[80]

Charged chemically modified surfaces act by direct contact between the antibacterial agents and the bacterial cell wall.[81,82] The head groups of phospholipids in the bacterial cellular membranes are negatively charged. Surfaces containing quaternary ammonium groups or primary to tertiary ammonium cations contain a positively charged nitrogen atom. This interacts with the negatively charged cell membrane causing a disturbance in the lipid

bilayers and a subsequent leakage in potassium ions.[83] As a result, bacterial cells lose their physiological functions and die.

Therefore, positively charged surfaces attract bacteria and negatively charged ones should repel them. However, attraction forces such as hydrophobic interactions (e.g., low surface energy) and van der Waals forces can overcome the electrostatic repulsion between bacteria and anionic surfaces.[80,84] Destabilizing interactions between negatively charged surfaces and bacterial cells can also be overcome by bacterial extracellular organelles including flagella, fimbriae curli, and pili, as they promote adhesion. [80,85]

Antibacterial surfaces have been categorized in the literature based on their mechanism of action.[86] There are three main approaches to design antimicrobial surfaces.[87] The first strategy focuses on preventing the initial attachment of bacteria by a so-called anti-biofouling or anti-adhesion effect. This is achieved by modifying the physicochemical properties of the surface such as hydrophobicity, topography, surface energy and roughness (Figure 12).

The second approach focuses on designing leaching surfaces that release antibacterial agents or inorganic metal ions from the surface over a period.[87] This approach has some disadvantages, because the residual amounts of antimicrobial leftover to the surrounding may cause adverse human health and environmental effects.[88,89] Also, these surfaces have a limited life span due to the gradual release of the antimicrobial agents.

The third approach aims to overcome these problems by covalently immobilizing antibacterial agents onto surfaces to kill bacteria upon contact. The covalent linkage forms stable and reliable antimicrobial surfaces without releasing active compounds to the environment, thus this approach minimizes environmental pollution.

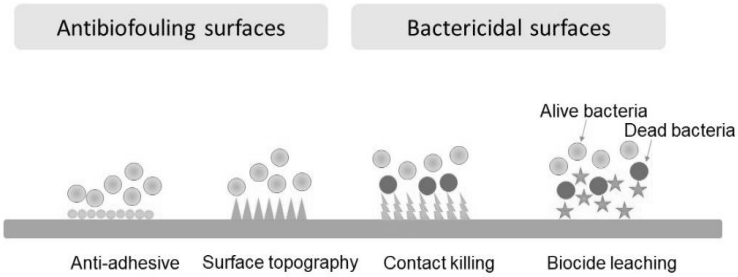

Figure 12 Examples of approaches used to design antibacterial surfaces. Antibiofouling surfaces repel bacterial cells from attaching by creating unfavorable conditions. Bactericidal surfaces kill bacterial cells upon contact.

Biodegradable polymeric materials have great potential in advancing biomedical applications.[90] While designing biodegradable biomaterials, different properties are considered, including biocompatibility, degradability, good mechanical properties and processability for designed applications.

Different polymers of synthetic or natural origin have been used for biomedical applications. Examples of the most widely used synthetic polymers include polyphosphazenes, polyacetals, polyphosphoesters, polyanhydrides, polycaprolactone and poly(orthoesters).[90] Even though these polymers fit functional demand, most of them are complex to synthesize, possess weak mechanical properties or have limited degradation.

Plant- and animal-based natural polymers, such as hyaluronic acid, chondroitin sulfate, cellulose, chitin and chitosan are widely used in biomedical applications.[91] In general, natural polymers are biocompatible, have excellent biodegradability, are cost-effective and easy to obtain in large amounts.[92] Recently, cellulose has been emerging as a promising natural and renewable polymer for biomedical applications.[93] This is due to its low cost, excellent mechanical properties, biodegradability, biocompatibility and low toxicity.

2.2.1 CELLULOSE NANOFIBERS

Cellulose **61** is a renewable raw material with a wide capacity for chemical modifications.[94] It is the most abundant polymer on earth with an annual production of 1.5×10^{12} tons produced from wood pulp and cotton. Cellulose is composed of repeating D-glucose units linked together by β-1,4 linkages with the formula $(C_6H_{10}O_5)_n$ where *n* is the degree of polymerization (Figure 13). Cellulose is 44.4% carbon, 49.4% oxygen and 6.2% hydrogen.[95] Cellulose has crystalline and amorphous regions in its structure with accessible hydroxyl groups on its surface.[96] Thus, cellulose is hydrophilic, and it swells in water. As cellulose is non-toxic and widely available, it has been used for a wide range of applications. Recently, the interest in the hydrophobization of cellulose has increased as a mean to explore its use in new applications.[97] Hydrophobicity of cellulose is measured by depositing a water droplet on its surface and assessing its contact angle (CA). In general, a material is considered hydrophobic when the CA is higher than 90°.[98]

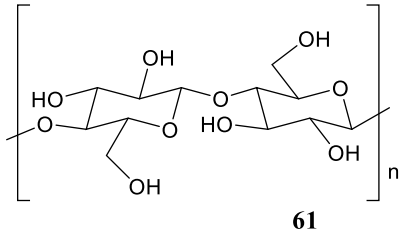

61

Figure 13 The chemical structure of cellulose (adapted from Klemm et al. 2005).[94]

Cellulose nanofibrils (CNF) are prepared mechanically via high shearing of cellulose fibers to achieve length in micrometric range and width in the nanometric range.[99] After shearing, the mass is homogenized at high pressure. This process provides entangled cellulose nanofibers with alternating amorphous and crystalline regions.

The nanoscale provides the CNF with an expanded uniform surface area where the hydroxyl groups on its structure can be chemically modified to create value-added advanced materials. Robust and solvent-resistant thin films can be made of CNF with excellent barrier properties to grease and atmospheric oxygen.[100] Those films represent a great platform for chemical modification to create functional materials. Different studies have focused on preparing nanocellulose with antimicrobial properties.[101,102,103,104] The most common methods to design non-leaching antibacterial nanocellulose surfaces have focused on hydroxyl substitution or other covalent surface modification reactions.[105] Esterification and silanation are commonly used modification methods. Various compounds have been used to esterify cellulose to produce high-performance active materials with antimicrobial properties.

Saini and colleagues modified the surface of nanocellulose with the β-lactam antibiotic benzylpenicillin (Figure 13).[106] The hydroxyl groups of the nanocellulose were reacted with the carboxyl group of the thiazolidine ring of benzylpenicillin. The esterification rendered relatively hydrophobic films with CA 89° ± 10°. The modified films were assessed for their antimicrobial activity against *S. aureus* and *E. coli* after a 24-h incubation. The modified nanocellulose exhibited strong activity against *S. aureus* as it reduced the number of viable staphylococci by 3.5 log units. However, benzylpenicillin-grafted nanocellulose was not active against *E. coli*. The research group speculated that this may be because penicillin acts on the bacterial cell wall. Gram-negative *E. coli* has an outer layer of lipopolysaccharide (LPS) that prevents the access of penicillin to the cell wall.

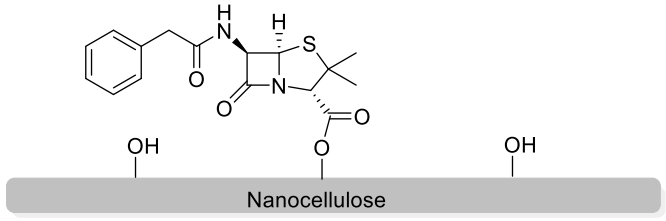

62

Figure 14 Benzylpenicillin-grafted nanocellulose.

Surface functionalization of cellulose nanocrystals (CNC) with resin acids provides the cellulose with hydrophobic and antimicrobial properties. de Castro and colleagues esterified the surface of CNC with rosin, a bio-based mixture of abietic and pimaric-type resin acids (Figure 15).[107] The research group tested the antimicrobial activity of neat and rosin-grafted CNCs on Gram-negative *E. coli* and Gram-positive *Bacillus subtilis*. The modified CNC exhibited good antibacterial activity against *B. subtilis* and weak activity against *E. coli*, indicating that the Gram-positive bacteria are more sensitive to rosin. The authors explained that modified CNC most likely reacts with the outer membrane of the bacteria. They added that the differences in the

structure of the cell wall between Gram-positive and Gram-negative bacteria would explain the selectivity of modified CNC.

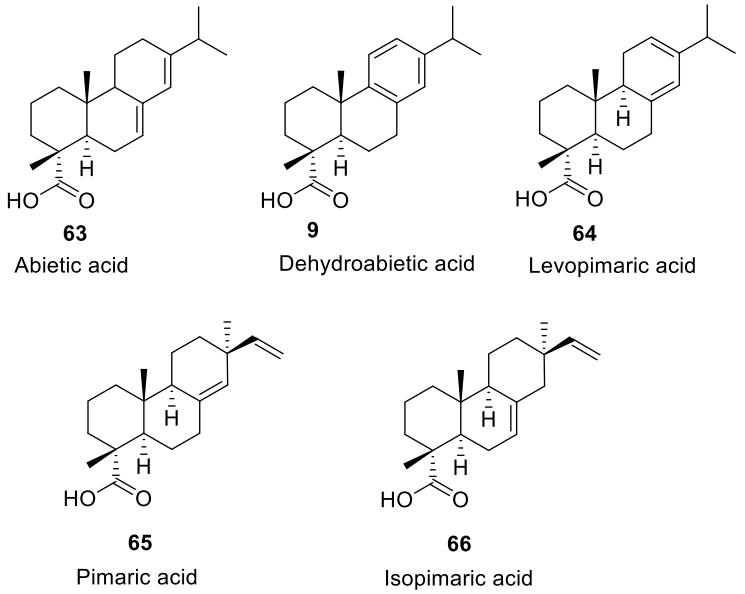

Figure 15 The most representative diterpene resin acids of the coniferous rosin.

In another study, Hassanpour et al. modified the surface of CNF with siloxane-linked phenanthridinium iodide and developed hydrophobic, non-leaching antibacterial films with different degrees of substitution.[87] First, the antibacterial agent (3-trimethoxysilylpropyl)phenanthridinium iodide (TMSPhI) was synthesized by reacting (3-chloropropyl)trimethoxysilane and phenanthridine in the presence of potassium iodide. Then the hydroxyl groups of CNF were reacted with the trimethoxysilyl group of TMSPhI to yield CNF-TMSPhI (Figure 16). CA measurements showed that the modification rendered more hydrophobic films.

Additionally, the research group tested the antibacterial properties of CNF-TMSPhI films against *S. aureus* and *E. coli*. The antibacterial activity varied with respect to the amount of TMSPhI present on the surface. In general, the films exhibited strong bactericidal activities against *E. coli*, whereas *S. aureus* was less susceptible to CNF–TMSPhI. The exact mechanism of action was not completely elucidated. However, the authors concluded that *E. coli* is more negatively charged than *S. aureus* and it reacts more efficiently with the positively charged TMSPhI by electrostatic interaction.

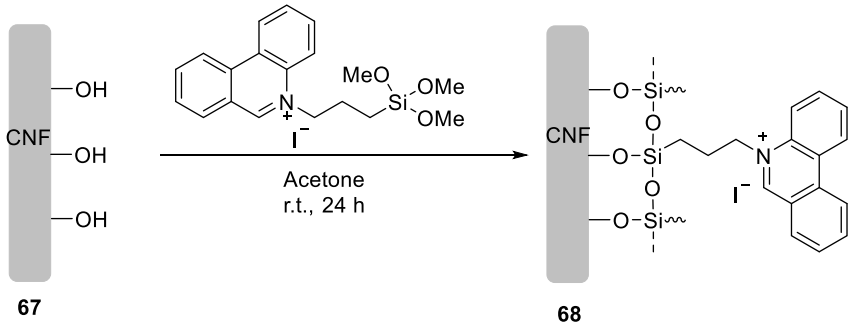

67 **68**

Figure 16 Covalent grafting of TMSPhI on the surface of CNF.

Currently, research on non-leaching antimicrobial nanocellulose is in the early stages and the number of studies dealing with this topic is low. Thus, further studies are needed to generate new classes of non-leaching biocompatible cellulose with outstanding antimicrobial properties.

3 AIMS OF THE STUDY

This thesis has two aims. The first aim was to design and synthesize new nanocellulose-based antibacterial surfaces to limit bacterial spread and infection. The second aim was to reveal details of the antimicrobial and anti-biofilm activity of pyrimidine derivatives and to establish their potential as a new class of hit compounds for discovery of novel drugs to treat infections caused by Gram-positive resistant bacteria.

The research questions for the first aim can be summarized as following: Will the covalent linking of dehydroabietanes to CNF result in antimicrobial properties? Will the activity of the covalently bound compounds be like that of the unbound ones? How will the physical and chemical properties of CNF change after modification? The first hypotheses were that dehydroabietanes will gift CNF with antimicrobial properties and increase the hydrophobicity of the material. As the methods used to modify the CNF are gentle, the fibrous structure is supposed to keep its integrity. As the compounds will be bound to the CNF surface covalently, they will be locked in a specific orientation which can impact their antimicrobial activities.

The research question for the second aim of the study was: Will chemical modification of the pyrimidine core render a potential new class of hit compounds with antibacterial properties? Studies have shown that modified pyrimidines possess a wide spectrum of biological activities, among which are antimicrobial activities. Thus, the second hypothesis was that chemical modification of pyrimidines will provide hit compounds that have antibacterial and anti-biofilm activities.

3.1 OUTLINE

The main findings of this research are displayed in the included articles, summarized as follows:

- **Publication I** was devoted to the design and synthesis of novel non-leaching contact-active surfaces using nanocellulose and dehydroabietylamine as a model compound due to its commercial availability. Pre-made CNF films were activated with carboxymethyl cellulose, after which the compounds were covalently linked to the surface through amide bond formation. The study yielded anionic surfaces that combine enhanced hydrophobicity with excellent broad-spectrum antimicrobial activity, bearing low potential to spread resistance. The beneficial characteristics of the original CNF film such as mechanical strength, breathability and moisture buffering were retained.

- **Publication II** was a follow-up from the first study. Another class of contact-active surfaces was designed and synthesized using derivatives of naturally occurring dehydroabietic acid. Similarly, the study rendered anionic, biocompatible and non-leaching films with excellent antimicrobial properties. The antimicrobial activity was detailed further by including a model mimicking chronic wound conditions, showing that the films prevent biofilm formation and bacterial colonization. In addition, the films nurtured fibroblast growth at their surface, making them excellent platforms for biomedical applications. In this publication, we created the first fully sustainable and efficient antimicrobial CNF film, based on raw materials from nature.

- **Publication III** focused on the design and synthesis of a new class of 2,4,5,6-tetrasubstituted pyrimidines and the assessment of their antibacterial and anti-biofilm activities *in vitro*. We identified three active compounds that inhibited biofilm formation and disrupted already established biofilms of *S. aureus* with IC_{50} values ranging from 11.6 to 62.0 μM. Mechanistic studies showed that the compounds do not act on the bacterial cell wall but instead they bind to intracellular bacterial targets. Cytotoxicity assessment showed moderate cytotoxicity against human Hep2 cells at a concentration close to their pre-exposure IC_{50} values.

4 RESULTS AND DISCUSSION

4.1 THE SYNTHESIS OF DEHYDROABIETYLAMINE-BASED CNF

Surfaces are highly sensitive to microbial attachment, causing infection spreading and contamination in health and industrial sectors.[108] A common approach to develop antimicrobial surfaces is by developing biocide-releasing materials, which leach antimicrobials such as triclosan and silver to the environment. The spread of bioactive molecules to industrial goods is not desired in order to maintain product properties and limit resistance against bacteria.[109] Currently, there is a growing interest in sustainable contact-kill surfaces.

Cellulose is a fully renewable and biodegradable polymer with outstanding properties and mechanical strength. Getting cellulose microfibrils to the nanosized scale adds desired properties to the natural cellulose such as uniformity and large surface area.[110]

Herein, we present the design and synthesis of innovative antimicrobial CNF films using (+)-dehydroabietylamine, a commercially available diterpenoid that was previously shown to possess antimicrobial activity.[57,111] This was done by covalently binding the diterpenoid and its derivative onto CNF films. Furthermore, we demonstrate the results of the material characterization and the antibacterial assessment.

4.1.1 DESIGN AND SYNTHESIS

Surface modification was done by chemically grafting **8** and its synthetic derivative **70** onto the CNF surface in a two-step reaction (Figure 18). First, the surface of CNF was enriched with carboxyl groups required to react with the amino groups of **8** or **70**. The irreversible adsorption of sodium carboxymethyl cellulose (Na-CMC) onto CNF was done by stirring a 5-cm diameter circle of CNF in a 0.05 M/0.01 M solution of $CaCl_2$/$NaHCO_3$ in water containing Na-CMC, at 80 °C, for 4 h.

Carboxymethyl cellulose (CMC) is a cellulose derivative, which possesses anionic carboxyl groups on its surface. A previous study has shown that CMC irreversibly adsorbed onto the negatively charged cellulose in the presence of electrolytes and increased its surface charge density (increased the negative charge of cellulose).[112] In our reaction, the electrolytes help the CMC to approach the cellulose surface where irreversible adsorption happens guided by molecular/structural affinity.[113]

We covalently linked the carboxyl groups on the CNF surface to **8** and **70** to synthesize **72** and **73**, respectively through the formation of an amide bond. To synthesize compound **70** (Figure 17), we reacted purified **8** with *tert*-butyl

(3-bromopropyl) carbamate and Cs_2CO_3 in DMF for 24 h. The reaction produced a mixture of mono- and bis-alkylated amines, which after chromatographic purification gave pure **69**, in 14% yield. The *tert*-butoxycarbonyl protecting group was removed after treating the compound with TFA in dichloromethane for 1.5 h at 0 °C.

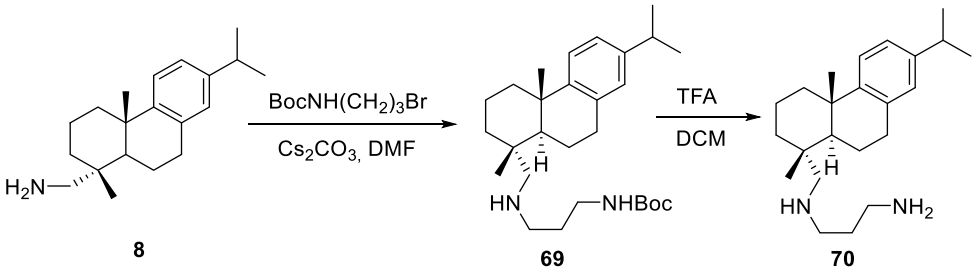

*Figure 17 The synthesis route of compound **70**.*

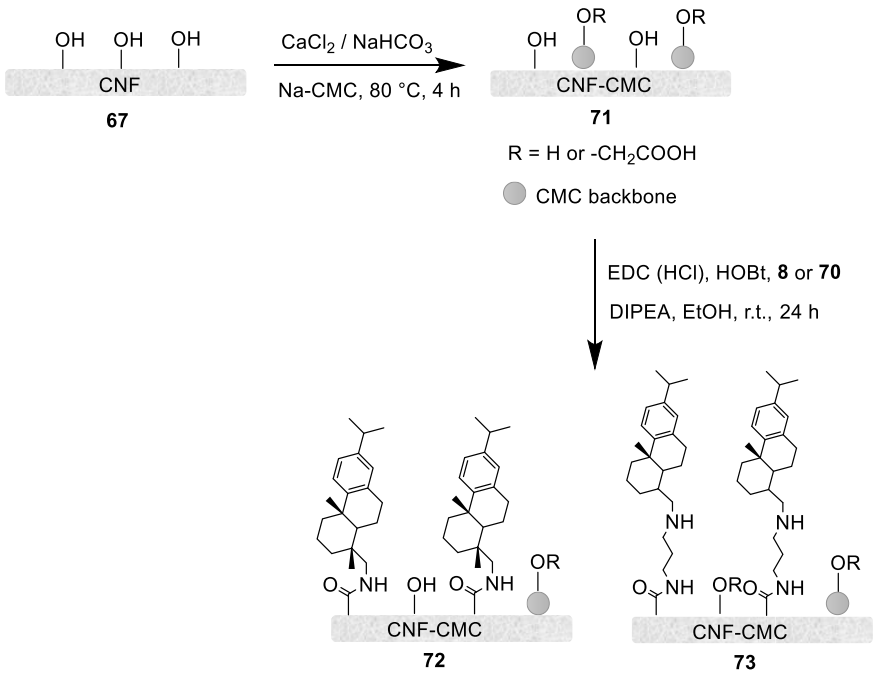

*Figure 18 Synthesis of **72** and **73**.*

4.1.2 SURFACE ANALYSIS AND CHARACTERIZATION

The successful modification of CNF was shown by the subsequent CA measurements. CNF and **71** are hydrophilic polymers (Publication I). The amidation of CNF-CMC reduced the water wettability and increased the hydrophobicity of the films. There was an apparent increase in the CA of the modified material (above 70°) compared to unmodified CNF (CA 31.4° ± 0.8°). This is expected as the covalently bound diterpenoids increased the carbon content at the CNF surface, suggesting a successful surface modification.

An insight into the chemical composition of the surfaces was explored via X-ray photoelectron spectroscopy (XPS; Table 5). The elemental surface analysis was done with low resolution wide survey scans. For more details, high resolution scans were done. The C 1s and O 1s content of modified and unmodified CNF were measured from three different locations per sample. Nitrogen content was determined via regional N 1s scans.

The XPS wide scan data of C 1s peak for unmodified and modified CNF is found from Figure 2 in Publication I. The main peaks corresponding to O and C are detected around 500 eV and 300 eV, respectively. The modified CNF showed new peaks at 400 eV corresponding to N atoms. Neither CMC nor cellulose has N in their chemical composition, thus, this change might have originated from our reaction. The surface O/C ratio for unmodified CNF is 0.74 while for **72** and **73** are 0.58 and 0.67, respectively. The lower C-O content for the modified CNF indicates the presence of carbon-rich **8** or **70** on the surface.

The high-resolution C 1s XPS spectra show that the intensity of C-C bond increases from 4.4% to 25% and 13.9% for unmodified CNF, **72** and **73**, respectively (Table 5). The increase in aliphatic carbon denotes the success of the modification.

*Table 5 XPS data for **72** and **73**.*

	Wide Scan Atomic Concentrations (%)				**High Resolution C 1s Carbon Fits**			
Sample	C 1s	O 1s	N 1s	Si 2p	C-C	C-O	O-C-O	O-C=O
CNF	60.7	39.3	0.0	0.0	4.4	74.5	19.2	1.9
72	67.0	32.1	0.9	0.0	25.0	58.4	14.9	1.7
73	62.2	35.9	1.3	0.7	13.9	66.5	17.2	2.5

The surface coverage was calculated for **72** and **73** by dividing the measured N and C content with the theoretical one. Based on the N content, compound **8** covered 20% of the CNF film surface. However, when based on the C-C content, the compound covered 25% of the surface. We estimated the surface coverage of **73** to be 18% based on N and 14% based on C-C. Overall, our results indicate a very low surface coverage.

We used atomic force microscopy (AFM) to investigate the nanoscale morphological details of unmodified and modified CNF. AFM height images

(Publication I, Table 3A) showed that the fibrous nanostructure of CNF remained unchanged after modification.

The mechanical properties of CNF and the ability to permeate vapor were not significantly changed by the modification. As displayed in Table S1 in Publication I, the tensile strength of **72** did not differ from unmodified CNF. However, modified CNF had a higher oxygen permeability at a low relative humidity (50%) than the unmodified one. This can be explained by the increase in surface hydrophobicity, which attracts more oxygen molecules to the films. Overall, the results show that the surface modification done was gentle.

To confirm that our changes occurred only on the surface, Fourier-transform infrared spectra were recorded for CNF before and after grafting. The results are shown in Publication I (Figure 3B). Unmodified CNF showed characteristic bands of cellulose at 3334 cm^{-1}, 2900 cm^{-1} and 1029 cm^{-1} for O-H, C-H and C-O-C, respectively. No significant differences were observed between modified and unmodified CNF indicating that the modification was done to the outermost surface.

4.1.3 EVALUATION OF THE ANTIBACTERIAL ACTIVITY

We investigated the ability of functionalized CNF to inhibit and kill different bacterial strains including Gram-positive *S. aureus*, Gram-negative *E. coli*, and methicillin-resistant *S. aureus* MRSA14TK301. Unmodified CNF was used as a control. As illustrated in Figure 19, the grafted materials exhibited remarkable activity against *S. aureus*. After 24 h of incubation, at 37 °C, a significant reduction of total cells from 10^5 colony-forming unit/mL (CFU/mL) bacterial suspensions was observed. Both **72** and **73** had obvious activity against MRSA with 91.3% and 98.4% reduction of total cells from the cell suspension, respectively. The film **72** succeeded in reducing total cells of *E. coli* from the bacterial suspension by 99.6% and **73** by 99.9%.

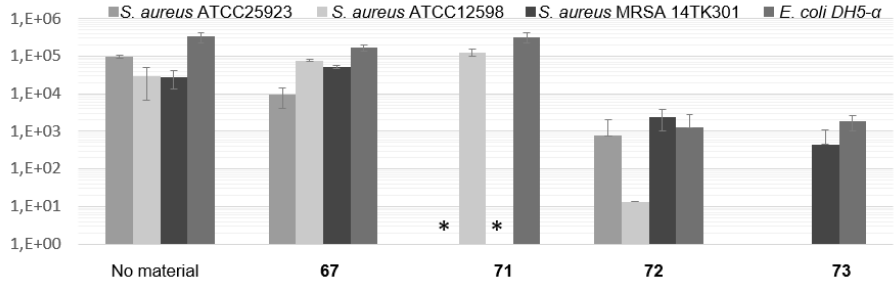

*Figure 19 Antimicrobial activity of **67**, **71**, **72**, and **73** in percent reduction of CFU/mL of ~10^5 bacterial suspensions. * not tested.*

We further investigated the effect of different solvents on the antimicrobial activity of **72** against *S. aureus* ATCC12598 (10^6 CFU/mL). After immersing the material in different solvents for 24 h at room temperature, we noticed that

except for treatments with dichloromethane (DCM) and 10% hydrochloric acid, **72** was not altered and the antimicrobial activity was retained after the exposure to different solvents (Table S2, Publication I). These results suggest that **8** did not leach from the surface and that our surface chemistry is stable when treated with different solvents.

As presented in the literature review, contact kill surfaces are created by binding biocides to them to gift them with contact-active antibacterial activity. To determine if **8** and **70** have the same antibacterial activities compared with their respective materials, we determined the minimal inhibitory concentration (MIC) values of **8** and **70** against *S. aureus* ATCC12598 and *E. coli* DH5α. In contrast to the materials, both compounds showed relatively weak antimicrobial activities (Table 6). Compound **8** had MIC values ranging between 40-50 µM while **70** had a slightly better MIC value of 30 µM. Incubation of 100 µM of **8** or **70** with the bacteria for 4 h showed bacterial cell death with ATP efflux indicating that the compounds caused disruption of the bacterial membrane.

*Table 6 The MIC values of **1** and **4** against S. aureus ATCC12598 and E. coli DH5α.*

	MIC (µM)	
Compound	*S. aureus* ATCC12598	*E. coli* DH5α
8	40	50
70	30	30

The main reported factors that affect the activity of contact-kill surfaces are charge, hydrophobicity, topography and chemical surface composition. For example, cationic surfaces interact with the negatively charged bacterial cell wall and disrupt it.[114] To understand better the interaction between bacteria and the material, we determined the surface charge of unmodified and modified CNF via stream current measurement (Figure 3C, Publication I). A background electrolyte of a 1 mM solution of KCl in water was used. The point of zero streaming was below pH 3 and reached an alkaline range, indicating that all the surfaces were negatively charged at the testing pH. As previously mentioned in the literature review, the electrostatic repulsion between the negatively charged surface of bacteria and anionic surfaces can be overcome by hydrophobic interactions and van der Waals forces.

Next, the changes occurring in *S. aureus* bacterial membrane were investigated after incubation with the materials (24 h) or compounds (100 µM, 1 h) using scanning electron microscope (SEM). As shown in Figure 4B (Publication I) no morphological changes were visible on the cells in contact with CNF and **72**. Obvious debris appeared for cells in contact with **73** or treated by **70** (Figure 20).

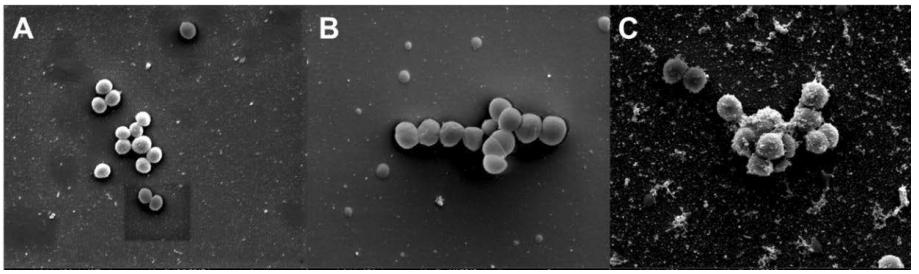

Figure 20 S. aureus ATCC12598 under scanning electron microscope. A: untreated S. aureus; B: S. aureus incubated with neat CNF for 24 h; C: S. aureus incubated with **73** *for 24 h.*

4.1.4 BIOCOMPATIBILITY ASSESSMENT

Unspecific cytotoxicity is a common concern related to the development of antimicrobial materials, especially if they have the potential to be used in biomedical applications. The FDA biocompatibility guideline states that hemocompatibility testing, especially hemolysis testing, should be considered for agents which could have direct contact with circulating blood.[115] We used hemolysis assay to determine if erythrocyte lysis is induced by contact with our surfaces. The film **72** showed a low level of hemolysis (0.9 ± 0.6) compared to that of the biocompatible[116] CNF (0), while **73** showed a higher level of hemolysis (6.5 ± 1.9) as shown in Table 2 (Publication I).

We also used cell viability assay to determine the ability of cells to survive on our films. Human skin fibroblasts were incubated with the films for 72 h. The cells colonized well on **72** to an extent comparable to unmodified CNF, which is considered biocompatible. However, only 3% of the cells colonized **73**, showing poor biocompatibility.

To our knowledge, this is the first study focusing on covalently linking antimicrobial diterpenes on CNF films via an amide bond. The success of the modification was confirmed by CA and XPS techniques. Even with low surface coverage, these antimicrobial surfaces proved to be very effective against Gram-positive and Gram-negative bacteria including the methicillin-resistant *S. aureus* MRSA14TK301 with good biocompatibility. Material characterization confirmed that the modified films retained the properties of the original CNF. Thus, diterpenes can be covalently bound to CNF to produce eco-friendly and inexpensive broad-spectrum antibacterial materials. The proposed mode of action together with the fact that the films are based on a new class of compounds, should account for low potential to spread resistance.

4.2 THE SYNTHESIS OF DEHYDROABIETIC ACID-BASED CNF

As previously reported, bacterial attachment and colonization cause biofilm-associated infections. *S. aureus* is found very frequently in biofilm-associated infections.[117] Diseases such as osteomyelitis, endocarditis, skin infections, urinary tract infection as well as implant-associated infections are all caused by *S. aureus* biofilm infection.

Dehydroabietic acid (DAA) is a diterpenoid found commonly in rosin.[118] Our previous studies showed that linking different amino acids to DAA produced potent anti-biofilm compounds, which were more potent than conventional antibiotics.[56] Inspired by these studies, we became interested in combining DAA derivatives with the biocompatible polymer CNF to extend structure-property and investigate the modes of action of abietane-CNF hybrids.

We designed and synthesized antimicrobial derivatives of DAA and covalently linked them to CNF films and further confirmed the success of the coupling reaction using time-of-flight secondary ion mass spectrometry (ToF-SIMS) analysis. The films were screened for their antimicrobial activity against Gram-positive and Gram-negative bacteria including the methicillin-resistant *S. aureus* MRSA. Biocompatibility studies assessed the proliferation of human fibroblasts cells on their surface and hemolysis assay determined whether they induce red blood cell lysis upon contact. Also, an *in vitro* artificial dermis model was used to investigate the antibacterial activity of compounds and materials in wound-like conditions.

4.2.1 DESIGN AND SYNTHESIS

Compound **84** bears a methyl ester at C18 while **85** has a cyclohexyl-L-alanine moiety in the same position. The compounds were synthesized by methylation of **9** or coupling with methyl ester hydrochloride of β-cyclohexyl-L-alanine, respectively (Figure 21). The Friedel-Crafts acylation of the aromatic ring C of the compounds was done by reacting them with acetyl chloride and aluminium chloride in dichloromethane to give **76** in 89% yield and **77** in 56% yield. The Baeyer-Villiger oxidation of the acetyl-linked diterpenes was done by reacting them with peracetic acid (36-40 wt.%) in AcOH to yield **78** and **79**. Conversion of **78** and **79** to **80** and **81**, respectively, was done by letting the compounds react with K_2CO_3 in MeOH for 35 min. The hydroxyl groups of phenols were reacted with *tert*-butyl (3-bromopropyl) carbamate in the presence of Cs_2CO_3, to yield **82** and **83**.

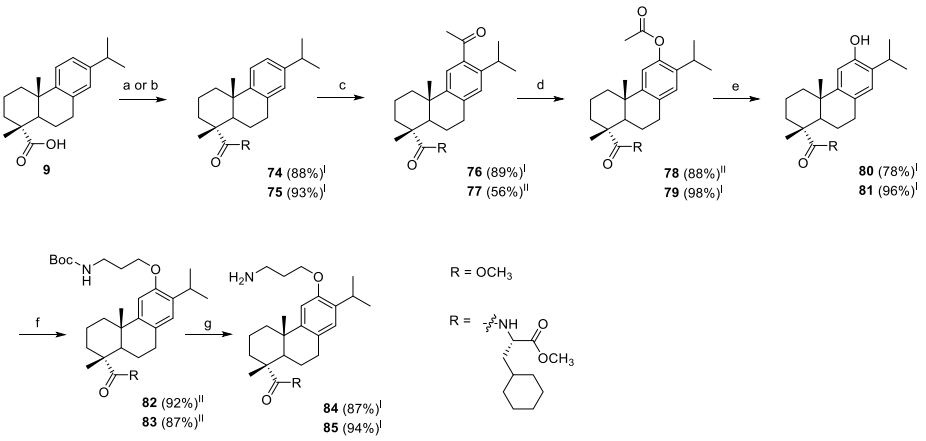

*Figure 21 Synthesis of **84** and **85**. Reagents and conditions: a. CH_3I, K_2CO_3, DMF, r.t. for **74**; b. EDC·HCl, DIPEA, HOBt, β-cyclohexyl-L-alanine methyl ester hydrochloride DMF, r.t., 24 h for **75**; c. AcCl, CH_2Cl_2, 0 °C to r.t.; d. AcOOH/AcOH, CH_2Cl_2, r.t; e. K_2CO_3, MeOH, r.t.; f. tert-butyl (3-bromopropyl) carbamate, Cs_2CO_3, DMF, r.t.; g. TFA, CH_2Cl_2, 0 °C. I Crude yield. II Yield after chromatographic purification.*

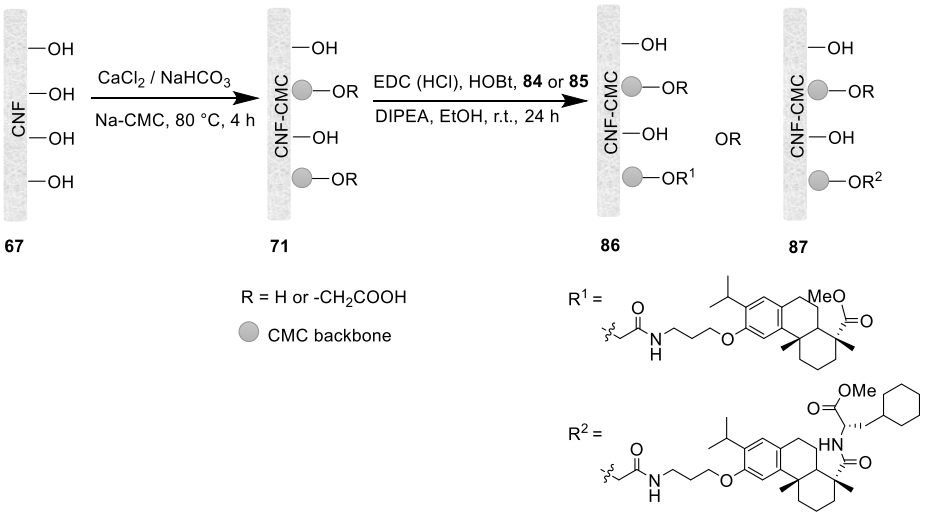

*Figure 22 Synthesis of **86** and **87**.*

The compound *tert*-butyl (3-bromopropyl) carbamate was synthesized by reacting 3-bromopropylamine hydrobromide with di-*tert*-butyl dicarbonate in the presence of triethylamine in DCM. Finally, the amino groups of **82** and **83** were deprotected by stirring the compounds with TFA in DCM to yield the final compounds **84** and **85** in 87% and 94% yields, respectively. The CNF films were activated by the irreversible adsorption of Na-CMC prior to linking **84** or **85** to its surface via carbodiimide coupling, to yield **86** and **87**, respectively (Figure 22).

4.2.2 SURFACE ANALYSIS AND CHARACTERIZATION

We have previously shown that XPS is an excellent technique for the characterization of modified CNF films (Publication I). Tables 7 and 8 present the changes in the chemical composition of the CNF surface before and after modification. The main elements identified were carbon, oxygen and nitrogen. We detected nitrogen on the modified surfaces following the amide bond formation compared to unmodified CNF. These results suggest successfully completed surface modifications. The C-C content on the surface of modified films was significantly higher due to the presence of dehydroabietic acid derivatives on the surface.

Table 7 Wide atomic scans (XPS) of neat and modified CNF films.

Wide Scan Atomic Concentrations (%)

Sample	C 1s	O 1s	N 1s	Si 2p
CNF	60.7	39.3	0.0	0
86	63.6	35.5	1.0	0
87	62.8	35.3	1.2	0.5

Table 8 High resolution C 1s carbon fits (XPS) for near and modified CNF.

High Resolution C 1s Carbon Fits

Sample	C-C	C-O	O-C-O	O-C=O
CNF	4.4	74.5	19.2	1.9
86	16.7	63.3	17.4	2.6
87	13.0	66.2	17.9	2.7

We calculated the surface coverage by dividing the measured C-C and N content with their corresponding theoretical values. The surface coverage for **86** was estimated to be 20% and 14% for **87** based on the C-C content. When calculated based on the N content, it was 30% and 25% for **86** and **87**, respectively.

In line with low surface coverage values, FTIR analysis did not show any changes when comparing the modified films to neat CNF (Figure 23). This proved that only the outermost surface was modified.

The CA measurements showed a more than two-fold increase in hydrophobicity of both **86** and **87** compared to neat CNF (Figure 24). The presence of **84** and **85** on the surface of CNF explains the increase in hydrophobicity due to the increase of surface carbon content.

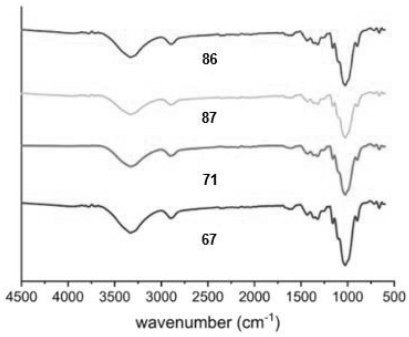

*Figure 23 FTIR spectra of **67**, **71**, **87** and **86** showing no differences between them.*

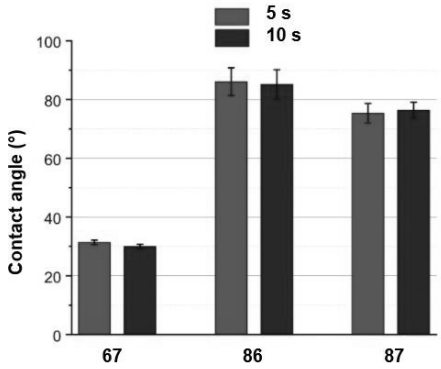

*Figure 24 Contact angle measurements at 5 and 30 seconds for **67**, **86** and **87**.*

To confirm the covalent coupling of **84** and **85** to CNF, we analyzed CNF, **71**, **85** and **87** using ToF-SIMS (Figures 3B and C, Publication II). This technique is commonly used to describe the chemical composition of solid surfaces. Compound **85** and **87** had a peak at *m/z* 541.5 in the positive ion mode. This peak was absent in CNF and CNF-CMC, indicating the presence of **85** on the surface of **87**. Another peak appeared at *m/z* 696.7 (Figure 3A, Publication II) which might correspond to a CMC unit attached to a fragment of **87**, where it is cleaved from the amide bond of ring A. This analysis confirms that our compounds are not adsorbed but covalently bound to the surface of CNF.

The streaming current measurements for **71** and **87** at varying pH showed that the material was anionic under the condition of the bacterial assay. The point of zero streaming was in acidic pH and reached a plateau of alkaline pH (Figure 3D, Publication II). The negative charge can be explained by the ionization of the carboxyl groups of CMC adsorbed onto the surface of CNF.

As the surface coverage of **87** is low, a similar electrokinetic fingerprint can be observed between **71** and **87**.

4.2.3 EVALUATION OF THE ANTIBACTERIAL ACTIVITY

The activity of the modified films was tested against different bacterial strains including Gram-negative *E. coli*, Gram-positive *S. aureus* and methicillin-resistant *S. aureus* MRSA14TK301. Log reduction describes the number of live microbes eliminated.[119] One-log reduction translates to 10-fold or 90% reduction in the number of viable bacterial cells. The inclusion of **85** on the CNF surface resulted in a significant 4-log reduction of staphylococcal cells in suspension (Figure 4B, Publication II). Moreover, **87** was active against viable MRSA and *E. coli*, with 5 and 2-log reduction in viable bacterial counts, respectively. The film **86** showed weaker antibacterial activity against the tested bacteria.

In contrast to **87**, compound **85** showed moderate antimicrobial activity against *S. aureus* with MIC value 15 µM and no activity against *E. coli* even when tested at 400 µM. Compound **84** showed weak activity against *S. aureus* and *E. coli* with MIC values 60 and 139 µM, respectively. These results clearly indicate that the mode of action of the films is different from that of the compounds. The incubation of 7 × MIC concentration of **85** with *S. aureus* for a short time did not cause apparent cell lysis which indicates that it is a slow-acting compound (Figure 6A, Publication II).

SEM images showed the morphological changes of *S. aureus* after incubation with CNF, **85** or **87** for 24 h (Figure 7, Publication II). Bacterial cells appeared unharmed with smooth, uniform and clear edges when in contact with unmodified CNF. However, collapsed cells were observed for round *S. aureus* when in contact with **85** or **87**, which could be indicative of membrane lysis or poration.

We investigated the ability of **87** to resist bacterial colonization in the artificial dermis and biofilm models. In the biofilm model, after 24 h of UAMS-1 biofilm formation, a significant 2.5-log reduction in recovered CFU was observed for **87** when compared to the neat CNF (Figure 5A, Publication II). Furthermore, **87** was placed on top of an infected artificial dermis model that mimics chronic wound conditions. The dermis was infected with 1×10^4 CFU of *S. aureus* UAMS-1. After 24 h incubation, the modified CNF exhibited a clear 1.4-log unit reduction in recovered CFU compared to unmodified CNF (Figure 5C, Publication II).

4.2.4 BIOCOMPATIBILITY ASSESSMENT

Due to its remarkable activity, we selected **87** for further studies. As it showed robust antibacterial activity, its cytotoxicity against mammalian cells was evaluated (Figure 4C, Publication II). The film **87** showed a low hemolytic

rate (1.8%) when incubated with human erythrocytes for 1 h at 37 °C. Furthermore, the fibroblasts proliferate better on **87** than on the biocompatible CNF after 72 h incubation at 37 °C.

4.2.5 STUDIES OF THE MECHANISTIC ACTION

To gain a deeper insight into the mechanism of action of **87**, we tested it against a mutant strain of Gram-positive *Lactococcus lactis* (LAC471) devoid of the AcmA autolysin. Autolysins are lytic enzymes at the surface of the bacteria responsible for cell wall turnover. The film **87** was only 10-fold less active against the mutated strain than against the original one. These results show that the release of autolysin is likely not the sole mechanism of action. The anionic charge of **87** can also bind to specific positively charged proteins on bacterial cell walls such as cationic autolysins.[120] However, the existence of the β-cyclohexyl-L-alanine side chain had a great impact on the activity of **87** compared to that of **86**. Thus, the spatial orientation of **85** on the surface of CNF impacted the reaction of the surface with the bacteria.

Our study generated anionic non-leaching surfaces with broad-spectrum antimicrobial activity. Upon contact, the films reduced MRSA-viable cells by 4-5 log units, proving to be very efficient. Also, the films prevented bacterial colonization when tested in chronic wound like-conditions. Biocompatibility studies showed that fibroblasts proliferate on the surface of the films and very low level of hemolysis was observed. Our results highlight the value of CNF and dehydroabietic hybrid for biomedical applications.

4.2.6 POTENTIAL MODE OF ACTION

A close inspection of the modified CNF shows a heterogeneous surface where unreacted carboxyl groups provide the surface with hydrophilic properties and the linked diterpenes on the surface provide hydrophobic regions. This distribution of polarity provides our surfaces with imperfect amphipathicity, like that of biosurfactants (BS). BS are surface-active molecules produced by microorganisms with hydrophilic and hydrophobic moieties. According to the surface charge of their hydrophilic moiety, BS can be anionic, non-ionic, cationic, and amphoteric.[121] They are mainly divided into glycolipids, lipoproteins, phospholipids and polymers.[122] They exhibit their antimicrobial activity, primarily, by disrupting the plasma membrane or cell wall of bacteria.[123] Rhamnolipids (RL, Figure 25) are glycolipid biosurfactants composed of a hydrophilic rhamnose moiety and a hydrophobic lipid tail linked by O-glycosidic linkage.[124] They have been widely studied for their broad-spectrum antimicrobial properties. RL have anionic charge at neutral pH and non-ionic properties at acidic conditions.[125]

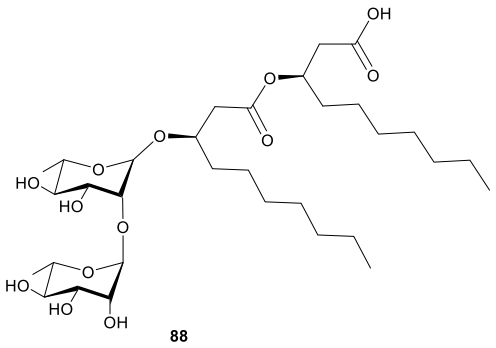

88

Figure 25 The structure of di-rhamnolipid (adapted form Kim et al. 2015).

A recent study evaluated the antibacterial activity of **88** against *S. aureus* biofilms established on polystyrene plates using broth or skimmed milk as the growth media.[125] The biofilm surface has charged groups, which promotes attractive or repulsive ionic interactions. In this study, the research group adjusted the solution of **88** to a neutral pH where the anionic form of **88** was dominant. The results revealed that RL activity depends on the biofilm matrix composition. RL disrupted 88.9% of the milk-based biofilm, probably due to the high carbohydrate content of milk-based biofilms. Biofilms grown in broth were less susceptible to **88**, as the biofilm was reduced by only 35%. The study concluded that **88** reacts with carbohydrates and promotes their solubilization.

Another study by Sotirova and colleagues investigated the effect of **88** on cell surface properties of *P. aeruginosa* NBIMCC 1390.[126] The effect of the biosurfactant was measured at concentrations above the critical micelle concentration (CMC; 153.7 μM, 461.0 μM) and below CMC (76.8 μM). CMC is the concentration of the surfactants, above which, micelles form.[127] Above CMC, the total LPS cellular content was reduced by 22%, while below CMC, LPS were not affected. Instead, the concentration of the outer membrane proteins (Opr F, Opr D, Opr J and Opr M) decreased.

A study investigated the physicochemical interactions between **88** and *P. aeruginosa* at a concentration of 461.0 μM, close to the CMC value 368.8 μM of **88**.[124] The results revealed that the protein and the carbohydrate content of the EPS of the biofilm decreased by 79.6% and 31.6%. RL interacted selectively with different EPS proteins and led to the reduction of amide groups and N sources on the membrane.

Similar to the anionic **88**, our surfaces could react with positively charged residues and carbohydrates on bacterial cell wall and modulate their activity. However, changes in compounds bound to the surface of CNF affected the activity as **86** had weaker activity compared to **87**. Thus, the spatial orientation of the bound molecules as well as the available functional groups participate in triggering the antibacterial activities. It is worth mentioning that compound **85** was active against the Gram-positive strains only while **87** exhibited activity against both bacterial species. Our results proved that the mode of action of

unbound compounds is clearly different from their respective surfaces, which likely reflects their inability to permeate cell membranes when physically bound onto CNF.

Our surfaces proved to be more active against Gram-positive *S. aureus* compared to Gram-negative *E. coli*. The main structural differences which distinguish Gram-positive bacteria from Gram-negative ones are a thicker peptidoglycan layer, the presence of teichoic acids and lipids and the absence of LPS.[128] The LPS consists of the lipid A, the core oligosaccharide and the O-antigen.[129] A study by Chaput and colleagues proved that the O-antigen neutralizes the negative charge of Gram-negative bacteria, which masks the charged residues required for charged antimicrobial peptides to exhibit activity.[130] Thus, a potential suppressor of the activity of our surfaces towards Gram-negative bacteria could be the charge masking ability of O-antigen which hampers the reaction of our surfaces with the bacteria. Another reason could be the selectivity of our surfaces to certain surface proteins, which exist mainly in *S. aureus* strains.

4.3 DESIGN AND SYNTHESIS OF 2,4,5,6-TETRASUBSTITUTED PYRIMIDINES

Biofilms form when microorganisms attach to surfaces, aggregate and form multicellular communities in a self-produced extracellular matrix.[131,69] Microorganisms form biofilms to protect themselves from environmental and chemical stresses. There are various problems associated with biofilm infections. Owing to their compact structure, biofilms are highly tolerant to the human immune response. They can also endure 10-1000-fold concentration of conventional antibiotics when compared to planktonic cells. For example, biofilms require a 600-fold increase in the concentration of chlorine, one of the most effective antibacterial agents, to be eradicated compared to planktonic cells. The rapid rise of antibacterial resistance combined with the lack of new antibiotic classes lead to hard-to-treat biofilm-related infections.

Pyrimidines are heterocyclic nitrogenous aromatic compounds with wide occurrence in nature.[132] As presented in the literature review, various studies have shown the relevance of pyrimidines in the development of new antibacterial agents. Aiming towards finding new antibacterial and anti-biofilm candidates, we screened a library of multi-substituted pyrimidines, against planktonic cells as well as against biofilm formation of *S. aureus* ATCC 25923 at 400 µM (Publication III, Table S1). We identified the hit compound **89** which inhibited biofilm formation by 91% (Figure 26). Based on these findings, we designed and synthesized two sets of 2,4,5,6-tetrasubstituted pyrimidines and optimized their potency.

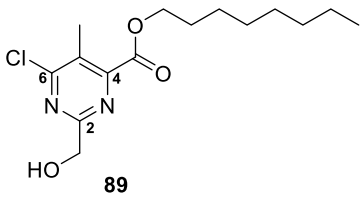

89

M.W. = 314.81 g·mol-1
cLogP = 3.2

Inhibition: Planktonic phase = 89%
Biofilm pre-exposure = 91%

*Figure 26 The chemical structure of the hit compound **89** and the inhibition percentage of the bacterial viability of S. aureus ATCC 25923, at 400 μM.*

4.3.1 Design and synthesis

Inspired by the hit molecule **89**, we designed two sets of compounds. Our design focused on the chemical modification of C2, C4 and C6 positions of the pyrimidine core. The first set had different linear alkyl substituents in position C4 with different lengths (2, 4 or 8) or a 3-(trifluoromethyl)benzyl substituent. A free or a *p*-methoxyphenyl (PMP)-protected hydroxymethyl moiety in C2 and Cl, Br or OH in position C6. Guided by the bioactivity testing of the set I and aiming to enhance the potency, we synthesized a second set of compounds. All compounds of set II had free hydroxymethyl moiety in position C2. Position C4 had either and 1-heptyl or 1-nonyl ester and fluoride in C6 (Figure 27). The most active compounds were selected for further studies.

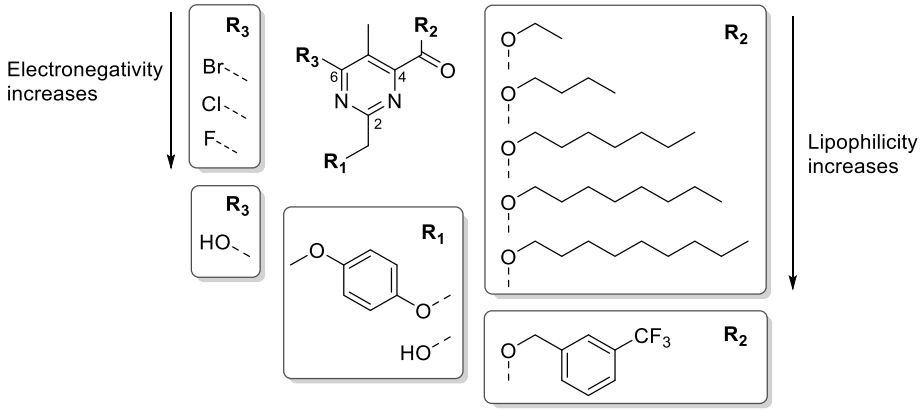

Figure 27 Design rationale of 2,4,5,6-tetrasubstituted pyrimidine scaffolds.

As previously reported,[133] we prepared compound **92** by reacting diethyl oxalpropionate (**90**) with 2-(4-methoxyphenoxy)acetamidine hydrochloride

(**91**), in the presence of triethylamine (TEA) in absolute ethanol. To assess the effect of different substituents on C4, we reacted **92** with different alcohols including 1-butanol, 1-heptanol, 1-octanol, 1-nonanol, or 3-(trifluoromethyl)benzyl alcohol in the presence of a catalytic amount of sulfuric acid to make **93b-f**. Except for 3-(trifluoromethyl)benzyl alcohol, the transesterification reaction yielded the disubstituted derivatives **94b**–**e** as side products. To examine the effect of different halogens on C6, we reacted the intermediates **92** and **93b**–**f** with phosphoryl bromide or phosphoryl chloride, in *N*,*N*-dimethylformamide (DMF) to yield **96a**–**e** and **97a**–**f**, respectively. Compound **97e** was converted to **98e** when stirred with KF and *n*-tetrabutylammonium bromide (TBAB) in sulfolane, as previously reported.[134] Finally, the *p*-methoxyphenyl (PMP) protective group was removed by an oxidative cleavage reaction by stirring **94b**–**e** and **96a**–**e**, **97a**–**f**, **98e**, and with ceric ammonium nitrate (CAN) in MeCN/H_2O to yield **95b**, **95d**, **99a**–**e**, **89, 100a-c, 100e-f** and **101e**, respectively, in 12-75% yield (Figure 28).

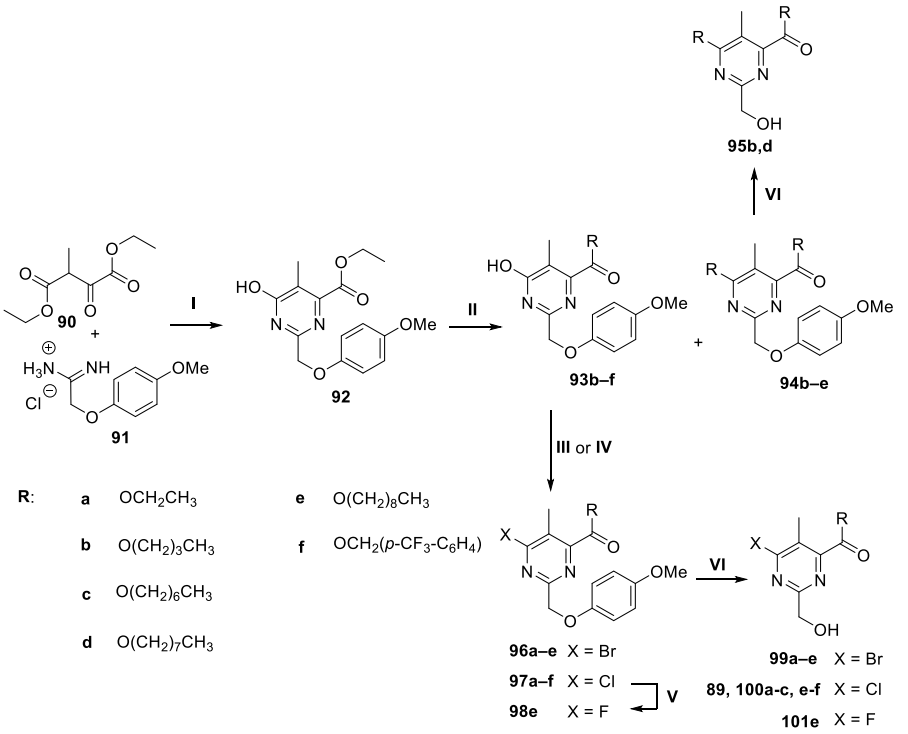

Figure 28 Synthesis of 2,4,5,6-tetrasubstituted pyrimidines. Conditions: (I) TEA, EtOH, reflux, (II) alcohol, H_2SO_4, 100 °C (III) $POBr_3$, DMF, 90 °C, (IV) $POCl_3$, DMF, 90 °C (V) KF, TBAB, sulfolane, 150 °C, (VI) CAN, MeCN/H_2O, -15 °C.

4.3.2 EVALUATION OF THE ANTIBACTERIAL ACTIVITY

To assess the activity of set I, we screened the compounds against the planktonic cells and prior-biofilm formation of *S. aureus* ATCC 25923, at 400 µM (Table S1, Publication III). Azithromycin was used as a reference. None of the compounds was more active than **89**. Of all the tested compounds, only **95b** and **99d** were active. They caused 88.3% and 83.4% inhibition of biofilm viability in the pre-exposure mode, respectively.

It was apparent that the PMP group did not contribute to the activity, as PMP-containing derivatives were all inactive. Replacing the Cl of **89** with Br decreased the activity. A plausible explanation is the difference in the electron-withdrawing properties or the size of the halogens. Bromine is less electronegative and bigger in size than chlorine.

Aiming to explore the structure-activity relationships (SAR) further, we designed and synthesized set II. As **89** and **99d** have an octyl ester in C4, we investigated the effect of ±1 carbon on the activity by introducing 1-heptyl (**99c**, **100c**) or 1-nonyl (**99e**, **100e**) in the same position. Fluorine is more electronegative and smaller than chlorine. We performed a chloride–fluoride replacement to assess its effect on the activity (**101e**). We tested **89**, **95b** and **99d** and our new set against two bacterial strains, *S. aureus* ATCC 25923 and *S. aureus* Newman at 100 µM.

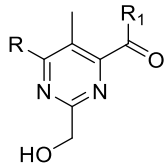

R = Cl, $R_1 = O(CH_2)_7CH_3$ **89**
R = Br, $R_1 = O(CH_2)_8CH_3$ **99e**
R = Cl, $R_1 = O(CH_2)_8CH_3$ **100e**

Table 9 The percentage of inhibition of bacterial viability of the most active compounds at 100 µM.

Cmpds (100 µM)	*S. aureus* ATCC 25923				*S. aureus* Newman	
	Planktonic phase		Biofilm pre-exposure		Biofilm pre-exposure	
	Mean	±SD	Mean	±SD	Mean	±SD
89	92.5	5.0	97.9	2.3	97.9	3.0
99e	94.3	2.1	98.1	0.1	99.8	0.1
100e	92.4	3.7	99.0	0.3	99.9	0.2
Azithromycin	99.6	0.1	97.0	0.4	99.3	0.1

Compounds exhibiting more than 50% inhibition in the pre-exposure assay are shown in Table 9. We identified **89**, **99e** and **100e** as the most active compounds as they exhibited good activities toward both bacterial strains.

Compound **101e** was devoid of activity compared to its analogue **89**. The replacement of 1-octyl with a 1-nonyl group in C4 resulted in comparable activity for the chlorinated analogue **100e** and enhanced activity for the brominated analogue **99e**. It is worth mentioning that **99d** showed a strain-specific activity, as it inhibited the biofilm of *S. aureus* ATCC 25923 by 51.7% but was inactive against *S. aureus* Newman.

We next explored the anti-biofilm potencies of **89**, **99e** and **100e** by determining their IC_{50} values in pre- and post-exposure modes of both *S. aureus* strains. We also measured their MIC values against planktonic cells. As displayed in Table 10, the three compounds successfully prevented biofilm formation and reduced the viability of existing biofilms. The compound **99e** was the most active with a MIC value 40 µM for both staphylococcal strains. Next, we calculated the logarithm of reduction of the viable cells caused by the three compounds at 100 µM, in both *S. aureus* strains. Both **99e** and **100e** displayed more than 2-log reductions while **89** displayed 3-log reductions (Figure 3, Publication III).

Table 10 The potency of the most active compounds.

Cmpds	***S. aureus* ATCC 25923**				***S. aureus* Newman**			
	Biofilms (IC_{50}, µM)			Planktonic bacteria	Biofilms (IC_{50}, µM)			Planktonic bacteria
	Pre	Post	Fold[a]	MIC (µM)	Pre	Post	Fold[a]	MIC (µM)
89	23.6	54.9	2.3	60	38.4	62.0	1.6	60
100e	16.8	51.8	3.1	60	37.3	44.8	1.2	60
99e	11.6	23.3	2.0	40	29.4	31.9	1.1	40

To assess whether the compounds have broad-spectrum activities, we tested them against two *P. aeruginosa* strains (ATCC 9027 and ATCC 15442) at 400 µM. The compounds were inactive against the tested Gram-negative strains as no significant reduction in viable cell counts was noticed after 24 h incubation.

4.3.3 CYTOTOXICITY EVALUATION

Unspecific cytotoxicity is a concern related to the development of new antibacterial agents. We tested our most active compounds against the human Hep2 cell line, at 100 µM (Table S3, Publication III). The compounds caused unspecific cytotoxicity when tested at 100 µM. However, when tested at 40 µM, a comparable concentration to their pre-exposure IC_{50} values, **89, 99e** and **100e** maintained 55%, 73% and 75% of cell viability, respectively.

4.3.4 STUDIES OF THE MECHANISTIC ACTION

To elucidate the possible mechanism of action, we performed membrane permeability studies by incubating the pre-formed biofilms of *S. aureus* ATCC 25923 with **89**, **99e** and **100e** for 2 h. Fluorescence imaging showed that none of the compounds disrupted the membrane integrity, indicating that they bind to intracellular targets.

The time-kill curve monitors the microbial viability in relation to the time and concentration of the antibacterial agent. We incubated different concentrations of **89** (0.5, 1 and 2 × the MIC value) with the viable cells of *S. aureus* ATCC 25923 during an 8-h period. No decrease in bacterial growth was observed for ½ × MIC and 1 × MIC during the 8-h incubation period. However, after 4 h, the compound exhibited a dose-dependent activity at 2 × MIC, decreasing the bacterial growth at a similar rate, comparable to that of azithromycin (Figure 4, Publication III). These results agree with the fluorescence imaging as compounds that bind to intracellular bacterial targets require longer response times.

This study highlights the value of pyrimidines as starting materials for the development of new antibacterial agents. Herein, we designed and synthesized new 2,4,5,6-tetrasubstituted pyrimidines and assessed their antimicrobial activities. We identified **89**, **99e** and **100e** as the most potent anti-biofilm agents as they effectively inhibited the biofilm formation and disrupted the established biofilms of two *S. aureus* strains. Our mechanistic studies showed that the compounds are slow-acting and that they do not target the bacterial membrane. Cytotoxic studies revealed that the compounds exhibited moderate cytotoxicity when tested against human Hep2 cells at concentrations closer to their pre-exposure IC_{50} values.

5 SUMMARY AND CONCLUSIONS

This thesis describes the design, synthesis and biological evaluation of antibacterial and anti-biofilm surfaces and compounds to target bacterial proliferation. Preventing the accumulation of microorganisms on surfaces limits the spread of infection. Drawbacks in the common strategies to design antibacterial surfaces include extreme complexity, the use of synthetic polymers and metal ions like silver, which are toxic to the environment.

Our study focused on developing new environmentally friendly and effective antibacterial and anti-biofilm surfaces based on cellulose nanofibrils. We synthesized four materials, which were characterized and tested for their antibacterial activities toward *E. coli*, *S. aureus* and methicillin-resistant *S. aureus*.

Our anionic materials showed clear and robust antimicrobial activity against all the tested bacterial strains. To establish their potential use in biomedical applications, we tested our most active material, **87** in both a biofilm and an artificial dermis model, which mimics the chronic wound environment. It successfully resisted bacterial colonization in both models. The biocompatibility studies showed that fibroblasts proliferated on the surface of **87** better than they did on the biocompatible CNF. Furthermore, only very minor hemolysis (1.8%) was caused by this film.

We speculate that the mechanism of action of our surfaces resemble that of the negatively charged biosurfactants. They bind to positively charged residues on the bacterial cell membrane and disturb them. Additionally, scanning electron micrographs showed damage to the cell wall of *S. aureus* after incubation with **87**. The unbound compounds showed different antimicrobial activity compared to their respective surfaces. The remarkable biocompatibility combined with the robust potency of our materials suggest their potential use as part of advanced biomaterials.

The WHO report on global surveillance of antimicrobial resistance states that antibiotic resistance is a real danger present in every continent. It is emerging faster than we are replacing current antibiotics. The most common strategy to develop new antimicrobial agents is to modify existing active analogues. As demonstrated in the literature review, resistance can occur to structurally similar compounds. Aiming to tackle this problem, we designed and synthesized a new set of 2,4,5,6-tetrasubstituted pyrimidines and tested them against planktonic cells and biofilms of *S. aureus*.

We identified **89**, **99e** and **100e** with the best antibacterial and anti-biofilm activities. They prevented biofilm formation and disrupted the already established biofilms with minimum inhibitory concentrations in the low micromolar range. Studies of the mechanistic action revealed that the compounds are slow-acting and that they do not target the bacterial cell wall. Cytotoxicity studies on human cells showed moderate cytotoxicity when

assayed at their pre-exposure IC_{50} values. Our study highlighted the value of pyrimidines as new interesting starting point for the development of small molecules to target resistant bacteria. Overall, our research illustrates alternative methods to fight bacterial resistance and limit the spread of infection.

REFERENCES

1. Moloney MG. Natural products as a source for novel antibiotics. Trends Pharmacol. Sci. 2016;37(8):689-701.
2. Shankar PR. Book review: Tackling drug-resistant infections globally. 7. Selangor: Monash University Malaysia, School of Pharmacy and Pharmaceutical Science; 2016. p. 110-111.
3. Chandy SJ, Naik GS, Balaji V, Jeyaseelan V, Thomas K, Lundborg CS. High cost burden and health consequences of antibiotic resistance: the price to pay. J. Infect. Dev. Countries. 2014;8(09):1096-1102.
4. World Health Organization. Antimicrobial resistance: global report on surveillance 2014, 2014, April. [Available from: https://www.who.int/drugresistance/documents/surveillancereport/en/, accessed 28 March 2020].
5. Zaman SB, Hussain MA, Nye R, Mehta V, Mamun KT, Hossain N. A review on antibiotic resistance: alarm bells are ringing. Cureus. 2017;9(6):e1403.
6. Clatworthy AE, Pierson E, Hung DT. Targeting virulence: a new paradigm for antimicrobial therapy. Nat. Chem. Biol. 2007;3(9):541-548.
7. Gould K. Antibiotics: from prehistory to the present day. J. Antimicrob. Chemother. 2016;71(3):572-575.
8. Munita JM, Arias CA. Mechanisms of antibiotic resistance. Virulence Mechanisms of Bacterial Pathogens, 5th Edition: Wiley Online Library; 2016. p. 481-511.
9. Rossolini GM, Arena F, Pecile P, Pollini S. Update on the antibiotic resistance crisis. Curr. Opin. Pharmacol. 2014;18:56-60.
10. Lebeaux D, Ghigo J-M, Beloin C. Biofilm-related infections: bridging the gap between clinical management and fundamental aspects of recalcitrance toward antibiotics. Microbiol. Mol. Biol. Rev. 2014;78(3):510-543.
11. Chandra H, Bishnoi P, Yadav A, Patni B, Mishra AP, Nautiyal AR. Antimicrobial resistance and the alternative resources with special emphasis on plant-based antimicrobials-a review. Plants. 2017;6(2):16.
12. Marceau AH, Bernstein DA, Walsh BW, Shapiro W, Simmons LA, Keck JL. Protein interactions in genome maintenance as novel antibacterial targets. PLoS One. 2013;8(3):e58765.
13. Johnsen L, Weigel C, von Kries J, Møller M, Skarstad K. A novel DNA gyrase inhibitor rescues *Escherichia coli* dnaAcos mutant cells from lethal hyperinitiation. J. Antimicrob. Chemother. 2010;65(5):924-930.
14. Chopra I, Roberts M. Tetracycline antibiotics: mode of action, applications, molecular biology, and epidemiology of bacterial resistance. Microbiol. Mol. Biol. Rev. 2001;65(2):232-260.
15. Santajit S, Indrawattana N. Mechanisms of antimicrobial resistance in ESKAPE pathogens. BioMed Res. Int. 2016;2016.
16. Silhavy TJ, Kahne D, Walker S. The bacterial cell envelope. Cold Spring Harbor Perspect. Biol. 2010;2(5):a000414.
17. Choi U, Lee C-R. Distinct roles of outer membrane porins in antibiotic resistance and membrane integrity in *Escherichia coli*. Front. Microbiol. 2019;10:953.

18. Webber M, Piddock L. The importance of efflux pumps in bacterial antibiotic resistance. J. Antimicrob. Chemother. 2003;51(1):9-11.
19. Pendleton JN, Gorman SP, Gilmore BF. Clinical relevance of the ESKAPE pathogens. Expert Rev. Anti-Infect. Ther. 2013;11(3):297-308.
20. Mulani MS, Kamble EE, Kumkar SN, Tawre MS, Pardesi KR. Emerging strategies to combat ESKAPE pathogens in the era of antimicrobial resistance: a review. Front. Microbiol. 2019;10:539.
21. Golkar Z, Bagasra O, Pace DG. Bacteriophage therapy: a potential solution for the antibiotic resistance crisis. J. Infect. Dev. Countries. 2014;8(02):129-136.
22. Percival SL, Suleman L, Vuotto C, Donelli G. Healthcare-associated infections, medical devices and biofilms: risk, tolerance and control. J. Med. Microbiol. 2015;64(4):323-334.
23. Ventola CL. The antibiotic resistance crisis: part 1: causes and threats. Pharm. Ther. 2015;40(4):277.
24. Quality AfHRa. Medical Expenditure Panel Survey: Household Component full year files 2002–2014, 2019, January. [Available from: https://meps.ahrq.gov/mepsweb/data_stats/download_data_files.jsp, accessed 3 June 2020].
25. Thorpe KE, Joski P, Johnston KJ. Antibiotic-resistant infection treatment costs have doubled since 2002, now exceeding $2 billion annually. Health Aff. 2018;37(4):662-669.
26. Lowy FD. Antimicrobial resistance: the example of *Staphylococcus aureus*. J. Clin. Investig. 2003;111(9):1265-1273.
27. Lakhundi S, Zhang K. Methicillin-resistant *Staphylococcus aureus*: molecular characterization, evolution, and epidemiology. Clin. Microbiol. Rev. 2018;31(4):1-103.
28. Stapleton PD, Taylor PW. Methicillin resistance in *Staphylococcus aureus*: mechanisms and modulation. Sci. Prog. 2002;85(1):57-72.
29. Chambers HF, DeLeo FR. Waves of resistance: *Staphylococcus aureus* in the antibiotic era. Nat. Rev. Microbiol. 2009;7(9):629-641.
30. Fair RJ, Tor Y. Antibiotics and bacterial resistance in the 21st century. Persp. Med. Chem. 2014;6:25–64.
31. Subramani R, Narayanasamy M, Feussner K. Plant-derived antimicrobials to fight against multi-drug-resistant human pathogens. 3 Biotech. 2017;172(7):1-15.
32. Dickmann P, Keeping S, Döring N, Schmidt AE, Binder C, Ariño-Blasco S, et al. Communicating the risk of MRSA: the role of clinical practice, regulation and other policies in five European countries. Front. Public Health. 2017;5(44):1-9.
33. Klevens RM, Morrison MA, Nadle J, Petit S, Gershman K, Ray S, et al. Invasive methicillin-resistant *Staphylococcus aureus* infections in the United States. J. Am. Med. Assoc. 2007;298(15):1763-1771.
34. Butler-Laporte G, De L'Étoile-Morel S, Cheng MP, McDonald EG, Lee TC. MRSA colonization status as a predictor of clinical infection: A systematic review and meta-analysis. J. Infect. 2018;77(6):489-495.
35. Vijayamohan N, Nair SP. A study of the prevalence of methicillin-resistant *Staphylococcus aureus* in dermatology inpatients. Indian Dermatol. Online J. 2014;5(4):441-445.
36. Lopes LP, Pio DPM, Reinato LAF, Gaspar GG, Prado MAd, Gir E. *Staphylococcus aureus* in nursing professionals and the microorganism's susceptibility profile to antimicrobials. Texto. Contexto. Enferm. 2017;26(2):1-8.

37. Roy R, Tiwari M, Donelli G, Tiwari V. Strategies for combating bacterial biofilms: A focus on anti-biofilm agents and their mechanisms of action. Virulence. 2018;9(1):522-554.
38. Branda SS, Vik Å, Friedman L, Kolter R. Biofilms: the matrix revisited. Trends Microbiol. 2005;13(1):20-26.
39. Lu L, Hu W, Tian Z, Yuan D, Yi G, Zhou Y, et al. Developing natural products as potential anti-biofilm agents. Chin. Med. 2019;14(11):1-17.
40. Moormeier DE, Bayles KW. *Staphylococcus aureus* biofilm: a complex developmental organism. Mol. Microbiol. 2017;104(3):365-376.
41. Briandet R, Herry J-M, Bellon-Fontaine M-N. Determination of the van der Waals, electron donor and electron acceptor surface tension components of static Gram-positive microbial biofilms. Colloids Surf. B. 2001;21(4):299-310.
42. Takahashi H, Suda T, Tanaka Y, Kimura B. Cellular hydrophobicity of *Listeria monocytogenes* involves initial attachment and biofilm formation on the surface of polyvinyl chloride. Lett. Appl. Microbiol. 2010;50(6):618-625.
43. Rutherford ST, Bassler BL. Bacterial quorum sensing: its role in virulence and possibilities for its control. Cold Spring Harb. Protoc. 2012;2(11):1-25.
44. Papenfort K, Bassler BL. Quorum sensing signal–response systems in Gram-negative bacteria. Nat. Rev. Microbiol. 2016;14(9):576-588.
45. O'Toole GA, Kolter R. Initiation of biofilm formation in *Pseudomonas fluorescens* WCS365 proceeds via multiple, convergent signalling pathways: a genetic analysis. Mol. Microbiol. 1998;28(3):449-461.
46. An D, Parsek MR. The promise and peril of transcriptional profiling in biofilm communities. Curr. Opin. Microbiol. 2007;10(3):292-296.
47. Hoffman LR, D'Argenio DA, MacCoss MJ, Zhang Z, Jones RA, Miller SI. Aminoglycoside antibiotics induce bacterial biofilm formation. Nature. 2005;436(7054):1171-1175.
48. Paredes J, Alonso-Arce M, Schmidt C, Valderas D, Sedano B, Legarda J, et al. Smart central venous port for early detection of bacterial biofilm related infections. Biomed. Microdevices. 2014;16(3):365-374.
49. Brooun A, Liu S, Lewis K. A dose-response study of antibiotic resistance in *Pseudomonas aeruginosa* biofilms. Antimicrob. Agents Chemother. 2000;44(3):640-646.
50. Ma H, Bryers JD. Non-invasive determination of conjugative transfer of plasmids bearing antibiotic-resistance genes in biofilm-bound bacteria: effects of substrate loading and antibiotic selection. Appl. Microbiol. Biotechnol. 2013;97(1):317-328.
51. Keeling CI, Bohlmann J. Diterpene resin acids in conifers. Phytochemistry. 2006;67(22):2415-2423.
52. Bohlmann J, Keeling CI. Terpenoid biomaterials. Plant J. 2008;54(4):656-669.
53. Singh B, Sharma RA. Plant terpenes: defense responses, phylogenetic analysis, regulation and clinical applications. 3 Biotech. 2015;5(2):129-151.
54. Guimarães AC, Meireles LM, Lemos MF, Guimarães MCC, Endringer DC, Fronza M, et al. Antibacterial activity of terpenes and terpenoids present in essential oils. Molecules. 2019;24(13):2471.
55. Zacchino SA, Butassi E, Di Liberto M, Raimondi M, Postigo A, Sortino M. Plant phenolics and terpenoids as adjuvants of antibacterial and antifungal drugs. Phytomedicine. 2017;37:27-48.

56. Manner S, Vahermo M, Skogman ME, Krogerus S, Vuorela PM, Yli-Kauhaluoma J, et al. New derivatives of dehydroabietic acid target planktonic and biofilm bacteria in *Staphylococcus aureus* and effectively disrupt bacterial membrane integrity. Eur. J. Med. Chem. 2015;102:68-79.
57. Fallarero A, Skogman M, Kujala J, Rajaratnam M, Moreira VM, Yli-Kauhaluoma J, et al. (+)-Dehydroabietic acid, an abietane-type diterpene, inhibits *Staphylococcus aureus* biofilms *in vitro*. Int. J. Mol. Sci. 2013;14(6):12054-12072.
58. González MA. Synthetic derivatives of aromatic abietane diterpenoids and their biological activities. Eur. J. Med. Chem. 2014;87:834-842.
59. Chabán MF, I Antoniou A, Karagianni C, Toumpa D, Joray MB, Bocco JL, et al. Synthesis and structure–activity relationships of novel abietane diterpenoids with activity against *Staphylococcus aureus*. Future Med. Chem. 2019;11(24):3109-3124.
60. Liu M-L, Pan X-Y, Yang T, Zhang W-M, Wang T-Q, Wang H-Y, et al. The synthesis and antistaphylococcal activity of dehydroabietic acid derivatives: Modifications at C-12. Bioorg. Med. Chem. Lett. 2016;26(22):5492-5496.
61. Gigante B, Silva AM, Marcelo-Curto MJ, Feio SS, Roseiro J, Reis LV. Structural effects on the bioactivity of dehydroabietic acid derivatives. Planta Med. 2002;68(08):680-684.
62. Sharma V, Chitranshi N, Agarwal AK. Significance and biological importance of pyrimidine in the microbial world. Int. J. Med. Chem. 2014;2014:1-31.
63. Brogden R, Carmine A, Heel R, Speight T, Avery G. Trimethoprim: a review of its antibacterial activity, pharmacokinetics and therapeutic use in urinary tract infections. Drugs. 1982;23(6):405-430.
64. Eliopoulos GM, Huovinen P. Resistance to trimethoprim-sulfamethoxazole. Clin. Infect. Dis. 2001;32(11):1608-1614.
65. Amyes S. Comparative antibacterial spectrum of trimethoprim and brodimoprim. J. Chemother. 1993;5(6):417-421.
66. Huang DB, Hawser S, Gemmell CG, Sahm DF. *In vitro* activity of iclaprim against methicillin-resistant *Staphylococcus aureus* nonsusceptible to daptomycin, linezolid, or vancomycin: a pilot study. Can. J. Infect. Dis. Med. Microbiol. 2017;2017:1-6.
67. Schneider P, Hawser S, Islam K. Iclaprim, a novel diaminopyrimidine with potent activity on trimethoprim sensitive and resistant bacteria. Bioorg. Med. Chem. Lett. 2003;13(23):4217-4221.
68. European Medicines Agency. Questions and answers on the withdrawal of the marketing authorisation application for Mersarex *iclaprim,* 2009, November. [Available from: https://www.ema.europa.eu/en/documents/medicine-qa/questions-answers-withdrawal-marketing-authorisation-application-mersarex-iclaprim_en.pdf, accessed 19 June 2020].
69. Powers J. Antimicrobial drug development–the past, the present, and the future. Clin. Microbiol. Infect. 2004;10:23-31.
70. Veeraswamy B, Madhu D, Dev GJ, Poornachandra Y, Kumar GS, Kumar CG, et al. Studies on synthesis of novel pyrido [2,3-*d*]pyrimidine derivatives, evaluation of their antimicrobial activity and molecular docking. Bioorg. Med. Chem. Lett. 2018;28(9):1670-1675.
71. Jang M-Y, De Jonghe S, Segers K, Anné J, Herdewijn P. Synthesis of novel 5-amino-thiazolo [4,5-*d*]pyrimidines as *E. coli* and *S. aureus* SecA inhibitors. Bioorg. Med. Chem. 2011;19(1):702-714.
72. Beyzaei H, Moghaddam-Manesh M, Aryan R, Ghasemi B, Samzadeh-Kermani A. Synthesis and *in vitro* antibacterial evaluation of 6-

substituted 4-amino-pyrazolo [3,4-*d*]pyrimidines. Chem. Pap. 2017;71(9):1685-1691.
73. Bai X-Q, Li C-S, Cui M-Y, Song Z-W, Zhou X-Y, Zhang C, et al. Synthesis and molecular docking studies of novel pyrimidine derivatives as potential antibacterial agents. Mol. Divers. 2019:1-12.
74. Zobell CE. The effect of solid surfaces upon bacterial activity. J. Bacteriol. 1943;46(1):39.
75. John A-K, Schmaler M, Khanna N, Landmann R. Reversible daptomycin tolerance of adherent staphylococci in an implant infection model. Antimicrob. Agents Chemother. 2011;55(7):3510-3516.
76. Tuson HH, Weibel DB. Bacteria–surface interactions. Soft Matter. 2013;9(17):4368-4380.
77. Oh JK, Yegin Y, Yang F, Zhang M, Li J, Huang S, et al. The influence of surface chemistry on the kinetics and thermodynamics of bacterial adhesion. Sci. Rep. 2018;8(1):1-13.
78. Bazaka K, Jacob MV, Crawford RJ, Ivanova EP. Efficient surface modification of biomaterial to prevent biofilm formation and the attachment of microorganisms. Appl. Microbiol. Biotechnol. 2012;95(2):299-311.
79. Arciola CR, Campoccia D, Speziale P, Montanaro L, Costerton JW. Biofilm formation in *Staphylococcus* implant infections. A review of molecular mechanisms and implications for biofilm-resistant materials. Biomaterials. 2012;33(26):5967-5982.
80. Renner LD, Weibel DB. Physicochemical regulation of biofilm formation. MRS Bull. 2011;36(5):347-355.
81. Tiller JC, Liao C-J, Lewis K, Klibanov AM. Designing surfaces that kill bacteria on contact. Proc. Natl. Acad. Sci. U. S. A. 2001;98(11):5981-5985.
82. Hasan J, Crawford RJ, Ivanova EP. Antibacterial surfaces: the quest for a new generation of biomaterials. Trends Biotechnol. 2013;31(5):295-304.
83. Gilbert P, Moore L. Cationic antiseptics: diversity of action under a common epithet. J. Appl. Microbiol. 2005;99(4):703-715.
84. Jucker BA, Harms H, Zehnder A. Adhesion of the positively charged bacterium *Stenotrophomonas* (*Xanthomonas*) *maltophilia* 70401 to glass and Teflon. J. Bacteriol. 1996;178(18):5472-5479.
85. Bullitt E, Makowski L. Structural polymorphism of bacterial adhesion pili. Nature. 1995;373(6510):164-167.
86. Li X, Wu B, Chen H, Nan K, Jin Y, Sun L, et al. Recent developments in smart antibacterial surfaces to inhibit biofilm formation and bacterial infections. J. Mater. Chem. B. 2018;6(26):4274-4292.
87. Hassanpour A, Asghari S, Lakouraj MM, Mohseni M. Preparation and characterization of contact active antibacterial surface based on chemically modified nanofibrillated cellulose by phenanthridinium silane salt. Int. J. Biol. Macromol. 2018;115:528-539.
88. Campoccia D, Montanaro L, Arciola CR. A review of the biomaterials technologies for infection-resistant surfaces. Biomaterials. 2013;34(34):8533-8554.
89. Lewis K, Klibanov AM. Surpassing nature: rational design of sterile-surface materials. Trends Biotechnol. 2005;23(7):343-348.
90. Ulery BD, Nair LS, Laurencin CT. Biomedical applications of biodegradable polymers. J. Polym. Sci. B Polym. Phys. 2011;49(12):832-864.
91. Aravamudhan A, Ramos DM, Nada AA, Kumbar SG. Natural polymers: polysaccharides and their derivatives for biomedical

applications. Natural and synthetic biomedical polymers: Elsevier; 2014. p. 67-89.
92. Balaji AB, Pakalapati H, Khalid M, Walvekar R, Siddiqui H. Natural and synthetic biocompatible and biodegradable polymers. Biodegradable and biocompatible polymer composites: processing, properties and applications. Woodhead Publishing series in composites science and engineering. Duxford: Woodhead Publishing 2017. p. 3-32.
93. Du H, Liu W, Zhang M, Si C, Zhang X, Li B. Cellulose nanocrystals and cellulose nanofibrils based hydrogels for biomedical applications. Carbohydr. Polym. 2019;209:130-144.
94. Klemm D, Heublein B, Fink HP, Bohn A. Cellulose: fascinating biopolymer and sustainable raw material. Angew. Chem., Int. Ed. 2005;44(22):3358-3393.
95. Jazaeri E, Zhang L, Wang X, Tsuzuki T. Fabrication of carbon nanofiber by pyrolysis of freeze-dried cellulose nanofiber. Cellulose. 2011;18(6):1481-1485.
96. Johansson L-S, Tammelin T, Campbell JM, Setälä H, Österberg M. Experimental evidence on medium driven cellulose surface adaptation demonstrated using nanofibrillated cellulose. Soft Matter. 2011;7(22):10917-10924.
97. Cunha AG, Gandini A. Turning polysaccharides into hydrophobic materials: a critical review. Part 1. Cellulose. Cellulose. 2010;17(5):875-889.
98. Feng L, Li S, Li Y, Li H, Zhang L, Zhai J, et al. Super-hydrophobic surfaces: from natural to artificial. Adv. Mater. 2002;14(24):1857-1860.
99. Zhang Y, Nypelö T, Salas C, Arboleda J, Hoeger IC, Rojas OJ. Cellulose nanofibrils. J. Renew. Mater. 2013;1(3):195-211.
100. Österberg M, Vartiainen J, Lucenius J, Hippi U, Seppälä J, Serimaa R, et al. A fast method to produce strong NFC films as a platform for barrier and functional materials. ACS Appl. Mater. Interfaces. 2013;5(11):4640-4647.
101. Yu H-Y, Chen G-Y, Wang Y-B, Yao J-M. A facile one-pot route for preparing cellulose nanocrystal/zinc oxide nanohybrids with high antibacterial and photocatalytic activity. Cellulose. 2015;22(1):261-273.
102. Missoum K, Sadocco P, Causio J, Belgacem MN, Bras J. Antibacterial activity and biodegradability assessment of chemically grafted nanofibrillated cellulose. Mater. Sci. Eng. C. 2014;45:477-483.
103. Saini S, Sillard C, Belgacem MN, Bras J. Nisin anchored cellulose nanofibers for long term antimicrobial active food packaging. RSC Adv. 2016;6(15):12422-12430.
104. Saini S, Belgacem MN, Bras J. Effect of variable aminoalkyl chains on chemical grafting of cellulose nanofiber and their antimicrobial activity. Mater. Sci. Eng. C. 2017;75:760-768.
105. Alavi M. Modifications of microcrystalline cellulose (MCC), nanofibrillated cellulose (NFC), and nanocrystalline cellulose (NCC) for antimicrobial and wound healing applications. e-Polymers. 2019;19(1):103-119.
106. Saini S, Belgacem N, Mendes J, Elegir G, Bras J. Contact antimicrobial surface obtained by chemical grafting of microfibrillated cellulose in aqueous solution limiting antibiotic release. ACS Appl. Mater. Interfaces. 2015;7(32):18076-18085.

107. de Castro DO, Bras J, Gandini A, Belgacem N. Surface grafting of cellulose nanocrystals with natural antimicrobial rosin mixture using a green process. Carbohydr. Polym. 2016;137:1-8.
108. Banerjee I, Pangule RC, Kane RS. Antifouling coatings: recent developments in the design of surfaces that prevent fouling by proteins, bacteria, and marine organisms. Adv. Mater. 2011;23(6):690-718.
109. Kaur R, Liu S. Antibacterial surface design–Contact kill. Prog. Surf. Sci. 2016;91(3):136-153.
110. Kalia S, Boufi S, Celli A, Kango S. Nanofibrillated cellulose: surface modification and potential applications. Colloid Polym. Sci. 2014;292(1):5-31.
111. Pirttimaa M, Nasereddin A, Kopelyanskiy D, Kaiser M, Yli-Kauhaluoma J, Oksman-Caldentey K-M, et al. Abietane-type diterpenoid amides with highly potent and selective activity against *Leishmania donovani* and *Trypanosoma cruzi*. J. Nat. Prod. 2016;79(2):362-368.
112. Laine J, Lindström T. Studies on topochemical modification of cellulosic fibres. Nord. Pulp Pap. Res. J. 2000;15(5):520-526.
113. Orelma H, Filpponen I, Johansson L-S, Laine J, Rojas OJ. Modification of cellulose films by adsorption of CMC and chitosan for controlled attachment of biomolecules. Biomacromolecules. 2011;12(12):4311-4318.
114. Carmona-Ribeiro AM, de Melo Carrasco LD. Cationic antimicrobial polymers and their assemblies. Int. J. Mol. Sci. 2013;14(5):9906-9946.
115. Food and Drug Administration. Use of International Standard ISO 10993-1, "Biological evaluation of medical devices - Part 1: Evaluation and testing within a risk management process" 2020, September [Available from: https://www.fda.gov/media/85865/download, accessed 15 June 2020].
116. Moohan J, Stewart SA, Espinosa E, Rosal A, Rodríguez A, Larrañeta E, et al. Cellulose nanofibers and other biopolymers for biomedical applications. A review. Appl. Sci. 2020;10(1):1-25.
117. Reffuveille F, Josse J, Vallé Q, Gangloff C, Gangloff SC. *Staphylococcus aureus* Biofilms and their Impact on the Medical Field. The Rise of Virulence and Antibiotic Resistance in *Staphylococcus aureus*: IntechOpen; 2017. p. 187-214.
118. Gu W, Wang S. Synthesis and antimicrobial activities of novel 1*H*-dibenzo[*a,c*]carbazoles from dehydroabietic acid. Eur. J. Med. Chem. 2010;45(10):4692-4696.
119. De Vries TA, Hamilton MA. Estimating the antimicrobial Log reduction: Part 1. Quantitative assays. Quant. Microbiol. 1999;1(1):29-45.
120. Chapot-Chartier M-P, Kulakauskas S. Cell wall structure and function in lactic acid bacteria. Microb. Cell Fact. 2014;13(S1):1-23.
121. Knepper TP, Berna JL. Surfactants: properties, production, and environmental aspects. Compr. Anal. Chem. 2003;40:1-49.
122. Bajpai Tripathy D, Mishra A. Sustainable biosurfactants. Encycl. Inorg. Bioinorg. Chem. 2011:1-17.
123. Ndlovu T, Rautenbach M, Vosloo JA, Khan S, Khan W. Characterisation and antimicrobial activity of biosurfactant extracts produced by *Bacillus amyloliquefaciens* and *Pseudomonas aeruginosa* isolated from a wastewater treatment plant. AMB Express. 2017;7(108):1-19.
124. Kim LH, Jung Y, Yu H-W, Chae K-J, Kim IS. Physicochemical interactions between rhamnolipids and *Pseudomonas aeruginosa* biofilm layers. Environ. Sci. Technol. 2015;49(6):3718-3726.

125. e Silva S, Carvalho J, Aires C, Nitschke M. Disruption of *Staphylococcus aureus* biofilms using rhamnolipid biosurfactants. J. Dairy Sci. 2017;100(10):7864-7873.
126. Sotirova A, Spasova D, Vasileva-Tonkova E, Galabova D. Effects of rhamnolipid-biosurfactant on cell surface of *Pseudomonas aeruginosa*. Microbiol. Res. 2009;164(3):297-303.
127. Rufino R, Luna J, Sarubbo L, Rodrigues L, Teixeira J, Campos-Takaki G. Antimicrobial and anti-adhesive potential of a biosurfactant Rufisan produced by *Candida lipolytica* UCP 0988. Colloids Surf. B. 2011;84(1):1-5.
128. Falk NA. Surfactants as Antimicrobials: A Brief Overview of Microbial Interfacial Chemistry and Surfactant Antimicrobial Activity. J. Surfactants Deterg. 2019;22(5):1119-1127.
129. Beaussart A, Beloin C, Ghigo J-M, Chapot-Chartier M-P, Kulakauskas S, Duval JF. Probing the influence of cell surface polysaccharides on nanodendrimer binding to Gram-negative and Gram-positive bacteria using single-nanoparticle force spectroscopy. Nanoscale. 2018;10(26):12743-12753.
130. Chaput C, Spindler E, Gill RT, Zychlinsky A. O-antigen protects gram-negative bacteria from histone killing. PLoS One. 2013;8(8):1-11.
131. Davies D. Understanding biofilm resistance to antibacterial agents. Nat. Rev. Drug Discov. 2003;2(2):114-122.
132. Lagoja IM. Pyrimidine as constituent of natural biologically active compounds. Chem. Biodivers. 2005;2(1):1-50.
133. Provenzani R, Tarvainen I, Brandoli G, Lempinen A, Artes S, Turku A, et al. Scaffold hopping from (5-hydroxymethyl)isophthalates to multisubstituted pyrimidines diminishes binding affinity to the C1 domain of protein kinase C. PLoS One. 2018;13(4):1-27.
134. Floersheimer A, Furet P, Manley PW, Bold G, Boss E, Guagnano V, et al., inventors; Novartis AG, Basel (CH), assignee. Diaryl urea derivatives useful for the treatment of protein kinase dependent diseases patent US 7,652,022 B2. 2010, January 26.